MODULATION OF LIPID DOMAIN FORMATION IN MIXED MODEL SYSTEMS BY PROTEINS AND PEPTIDES

Alexis Jean Oldham

A Thesis Submitted to the
University of North Carolina Wilmington in Partial Fulfillment
of the Requirements for the Degree of
Master of Science

Department of Chemistry and Biochemistry

University of North Carolina Wilmington

2008

Approved by

Advisory Committee

Dr. Sridhar Varadarajan

Dr. Richard Dillaman

Dr. Paulo Almeida
Chair

Accepted by

Robert D. Roer
Digitally signed by Robert D. Roer
DN: cn=Robert D. Roer, o=UNCW, ou=Dean of the Graduate School & Research, email=roer@uncw.edu, c=US
Date: 2008.05.19 09:33:33 -04'00'

Dr. Robert Roer
Dean, Graduate School

This thesis has been prepared in the style and format

consistent with the journal

Biochemistry

TABLE OF CONTENTS

ABSTRACT

The control of lipid domain formation in biological membranes has received limited consideration. This mechanism is quantitatively investigated using Monte Carlo computer simulations of a simple model system. Monte Carlo simulations are performed on a simple model system composed of phosphatidylecholine (PC), phosphatidylserine (PS), and cholesterol (Chol). Domain formation induced by binding of the phospholipid binding proteins, annexin A5 (A5) and the C2 protein motif is investigated. Simulations for models containing PC/PS lipids indicate that the addition of A5 does not induce lipid domain formation while binding of C2 greatly induces lipid domain formation. The addition of Chol to PC/PS systems was found to induce lipid demixing in the absence and presence of A5 and further enhance the ability of C2 to form PS domains. Incorporation of a preferential protein-protein interaction to PC/PS and PC/PS/Chol systems was found to further increase lipid demixing for all compositions.

Lipid domain formation is also investigated experimentally using fluorescence resonance energy transfer (FRET) in 1-Palmitoyl-2-oleoyl-*sn*-glycero-3-phosphocholine (POPC)/ sphingomyelin from porcine brain (BSM)/ Cholesterol (Chol) model systems. Studies have shown that these model systems contain lipid domains. The dependence of lipid domain size upon the addition of the transmembrane region of the linker for activation of T-cells (LAT), a protein believed to associate with lipid rafts, is investigated. When incorporated, LAT was found to insert into both the liquid-ordered (L_o) and liquid-disordered (L_d) regions indicating no lipid specificity. FRET between an acceptor/donor pair shown to not be affected by addition of LAT in POPC/BSM/Chol mixtures indicating that the presence of LAT does not affect the size of lipid domains.

ACKNOWLEDGEMENTS

I would like to thank the faculty and staff of the UNCW Department of Chemistry and Biochemistry for providing me with an excellent education. I would like to thank my committee members, Dr. Sridhar Varadarajan and Dr. Richard Dillaman, for their support and guidance throughout my research career and for enriching my learning experience.

Thanks to everyone in the Almeida lab for making each day so enjoyable. I will greatly miss each and every one of them. Thank you to Dr. Antje Pokorny Almeida for being my second advisor and friend.

A special thank you to my family and my fiancé, David Best, for always believing in me and for supporting me in all I have done. Their support and love means more to me than I could ever begin to explain.

Finally, I would like to thank Dr. Paulo F. Almeida for opening my eyes to the world of scientific research early in my academic career. I thank him for his guidance and patience throughout my studies. Without his help I would not be where I am today and for that I am forever grateful.

LIST OF TABLES

LIST OF FIGURES

INTRODUCTION

Domain models of cell membranes have been proposed based on the properties of lipids in model membranes. These models view lipid bilayers as "more mosaic than fluid" (1). The presence of lipid domains in model and biological membranes has become a significant aspect of the current understanding of membrane structure and function. In the late 1990's, it was suggested that a variety of cell membranes contain lipid rafts, microdomains rich in sphingomyelin (SM) and cholesterol (Chol) (2). Raft domains have received considerable attention because of their role in cell biology as platforms for the assembly of signal transduction protein complexes, cell polarity, and in trafficking and sorting of membrane-associated proteins (3). Propagation of signal transduction events typically involves protein-protein interactions. Such events would be greatly enhanced in both magnitude and specificity if the proteins and lipids involved were concentrated in the same domain rather than dispersed over many small, disconnected domains (4). It has been shown that in model systems of 1-Palmitoyl-2-oleoyl-*sn*-glycero-3-phosphocholine (POPC), porcine brain sphingomyelin (BSM), and Chol, raft/nonraft domains coexist as liquid-ordered (L_o) and liquid-disordered (L_d) domains (5) with SM/Chol making up the L_o domain because of their rigid structures and POPC making up the L_d domain. However, while attention has been focused on the orientation and role of lipid domains in the function of biological membranes, a clear understanding of the physical basis of raft domain formation has yet to be achieved (4).

Lipid Domain Regulation and Protein Binding

This research presents a quantitative investigation of lipid domain formation in terms of lipid-lipid, lipid-protein, and protein-protein interactions. The presence of stable domains in model membranes would be expected if the net difference in interaction between the lipids involved

were very large. However, in biological membranes these interactions are small enough to allow the lipid distribution to freely change. Differences in Gibbs free energies between different lipid species in model membranes are typically a few hundered calories per mole (6, 7). However, if there is a large number of molecules possessing such energies the interactions will be enhanced, which can result in lipid domain formation. Previous research with model membranes has demonstrated that small changes in the interaction between different lipid species can lead to dramatic changes in lipid distribution and induce lipid demixing (4). Also, changes in Gibbs free energies involved in protein-membrane interactions are typically much larger (several kilocalories per mole of protein) than lipid-lipid interactions (4). If such a protein is incorporated into a system, lipid clustering and protein-membrane interactions will be strongly coupled thermodynamically. The net strength of these interactions should be dependent on the lipid composition of the model membranes as well as the type of protein introduced to the system.

This study focuses on the regulation of lipid domains in mixed model systems containing phosphatidylserine (PS), phosphatidylcholine (PC), and Chol lipids. Eukaryotic cells contain various Ca^{2+} effector proteins that mediate cellular responses to changes in intracellular Ca^{2+} levels. One such family of proteins is formed by the annexins. Annexins are Ca^{2+}- and phospholipid- binding proteins that account for up to 2% of all intracellular proteins, with members expressed throughout the animal and plant kingdoms (8). They are characterized by their Ca^{2+} binding sites, which allow them to bind to negatively charged lipids in their Ca^{2+}-bound conformation. Structurally, each annexin consists of two principal domains: a conserved C-terminal protein core and a variable N-terminal head region (Figure 1). The conserved protein core is comprised of four repeats with each repeat containing five amphiphilic α-helices. The variability in the N-terminal region is believed to give the specificity in the Ca^{2+}-and

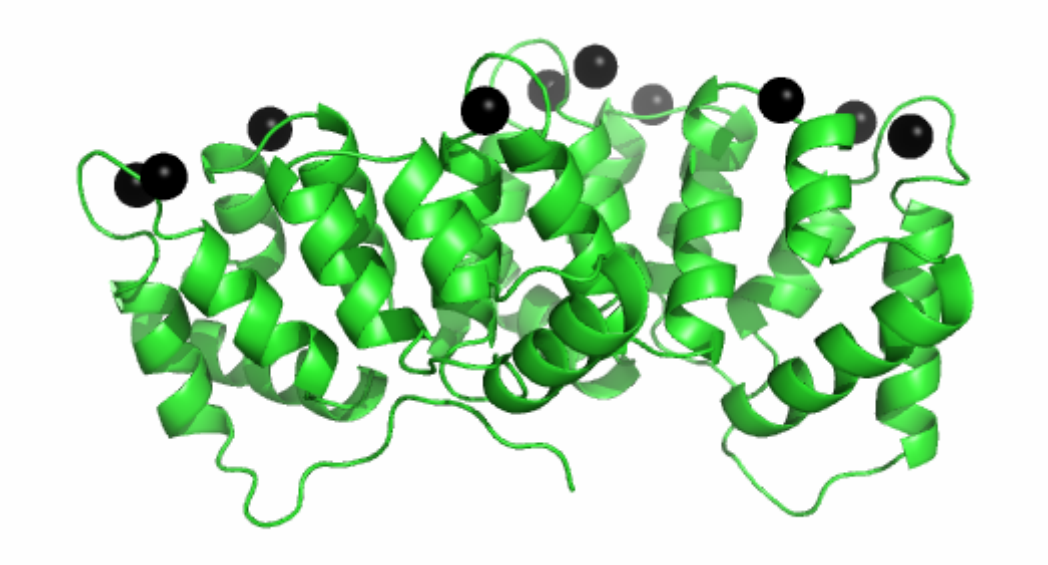

Figure 1. Structure of Annexin A5. Calcium ions are represented by black spheres.

phospholipid-binding ability of the annexins (8). Annexins have no detectable enzymatic function and recent findings have implicated a role for them in prostate cancer, pathogenic infections, and blood coagulation diseases (9). The affinity of annexins for Ca^{2+} and PS is highly conserved among species. Recent studies have indicated that annexin A5 (A5) forms clusters of trimers upon binding to membrane surfaces (10, 11). Such a clustering of proteins could magnify the overall ability of annexin to induce lipid domain formation. It is this apparent protein clustering ability and preferential binding to PS that suggests a possible function for annexins in lipid domain formation.

The lipid clustering ability of the annexin with the shortest N-terminus, annexin A5, was tested using Monte Carlo computer simulations of systems composed of various mixtures of PS and PC, and Chol. The lipid domain structure was investigated in the presence and absence of externally added protein. The Monte Carlo simulations are based on the idea that small lipid-lipid interactions can thermodynamically couple with stronger protein-membrane and protein-protein interactions and result in lipid domain formation.

To obtain a quantitative description of each system, estimates of the Gibbs free energy changes associated with protein-PC and protein-PS interactions were required. These values were obtained by the use of experimentally determined binding constants for each protein (12). Also required were estimates for all unlike lipid interactions, which have been previously determined (4). Results from these experiments were compared with those from the C2 domain motif of rat synaptotagmin I, a peripheral membrane binding motif found in an abundance of proteins implicated in eukaryotic signal transduction and cellular trafficking processes (4). Like annexin, the C2 motif is known to bind to negatively PS lipids in a Ca^{2+} dependent manner (4).

Dependence of FRET on Peptide Incorporation into POPC/BSM/Chol membranes

Simple model systems have been widely used as a means for monitoring lipid domain regulation for various lipid mixtures. Results obtained using these model systems help to shed light on interactions between different lipid species, peptides and proteins commonly found in biological membranes. One area of debate surrounding the use of simple model systems composed of only lipid mixtures is that such systems are not true representations of biological membranes. Such membranes contain not only many lipids species, but various types of proteins within the bilayer, thus, leading to speculation that experiments performed using these simple systems may lead to inaccurate findings.

This research monitors the incorporation an α-helical peptide into large unilamellar vesicles (LUVs) composed of POPC/BSM/Chol and its effect on lipid distribution. The peptide used for this study is an analogue of the transmembrane region of the linker for activation of T cells (LAT). LAT is found in the plasma membrane and is known to play an essential signaling role in T cells. It is speculated that LAT must associate with lipid rafts in order to function (13). Its structure consists of a short 3-residue extracellular domain, a single membrane-spanning domain, and an intracellular domain (13). In the present study, a short peptide with the sequence, EADWLSPVGLGLLLLPFLVTLLAALAVRARE, corresponding to residues 2–32 of murine LAT, will be utilized. This peptide includes the transmembrane domain and both acylation sites of LAT (14).

A current method for monitoring the regulation of lipid domains in simple model systems is the incorporation of lipid probes into the bilayer that act as a fluorescent energy transfer donor/acceptor pair. This process is known as fluorescence resonance energy transfer (FRET). In FRET, energy is directly transferred from one molecule to another without emission from the donor. For energy transfer to occur, the donor and acceptor molecules must have overlapping

emission and absorption spectra, and also be in close proximity. One such energy transfer pair is Marina Blue-1-palmitoyl-2-oleoyl-*sn*-glycero-3-phosphoethanolamine (MB-POPE) and 7-nitrobenz-2-oxa-1,3-diazole-1-palmitoyl-2-oleoyl-*sn*-glycero-3-phosphoethanolamine (NBD-POPE). The absorption spectra of MB-POPE and NBD-POPE in methanol, and the fluorescence emission spectra of MB-POPE and NBD-POPE in pH 7.5 buffer (Figure 2) illustrate that there is a large overlap between the emission of MB-POPE and the absorption of NBD-POPE. Thus, these two fluorophores are an excellent Förster energy transfer pair (5). FRET between these two probes was used to monitor the effect of addition of LAT to large unilamellar vesicles (LUVs) of various lipid mixtures.

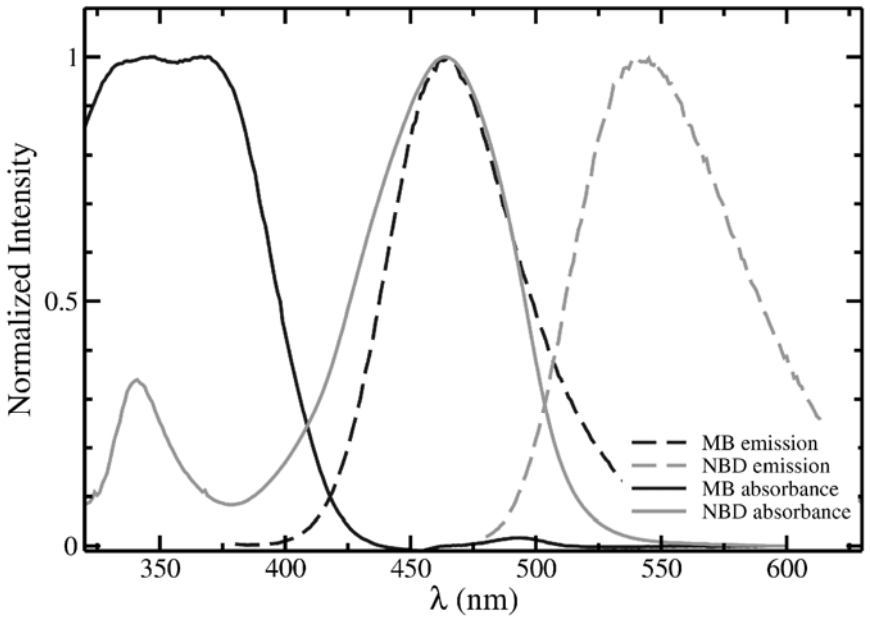

Figure 2. Normalized absorption and emission spectra of MB-POPE (black) and NBD-POPE (gray). Absorption spectrafor each fluorophore was recorded in methanol. Emission spectra were obtained in pH 7.5 buffer solution. Black lines correspond to the absorption (dashed) and emission (solid) spectra of MB-POPE. Gray lines correspond to the absorption (dashed) and emission (solid) spectra of NBD-POPE.

MATERIALS AND METHODS

Chemicals

1-Palmitoyl-2-oleoyl-*sn*-glycero-3-phosphocholine (POPC) and 1-palmitoyl-2-oleoyl-*sn*-glycero-3-phosphoethanolamine (POPE) in chloroform solution; sphingomyelin ((2S,3R,4E)-2-acylaminooctadec-4-ene-3-hydroxyl-1-phosphocholine) from porcine brain (BSM), in chloroform solution; and cholesterol (Chol), as powder, were purchased from Avanti Polar Lipids (Alabaster, AL). 4-Chloro-7-nitrobenz-2-oxa-1,3-diazole (NBD-Cl), 1-[[(6,8-difluoro-7-hyrdroxy-4-methyl-2-oxo-2H-1-benzopyran-3-yl)acetyl]oxy]-succinimidyl ester (Marina Blue-succinimidyl ester, MB-SE), and 7-methoxy coumarin (7-MC) were purchased from Molecular Probes/Invitrogen (Carlsbad, CA). Organic solvents (high-performance liquid chromatography/American Chemical Society (ACS) grade) were purchased from Burdick & Jackson (Muskegon, MI). Lipids and probes were tested by thin-layer chromatography (TLC) and used without further purification. An analogue of the LAT peptide with sequence, EADWLSPVGLGLLLLPFLVTLLAALAVRARE (substitutions of Trp for Ala^{4}, and Ala for $Cys^{26,29}$), corresponding to residues 2–32 of murine LAT, was purchased from Synbiosci (Livermore, CA).

Preparation of Large Unilamellar Vesicles

Large unilamellar vesicles (LUVs) were prepared by mixing appropriate amounts of lipids in 4:1 chloroform ($CHCl_3$) /methanol (MeOH) in a round bottom flask. When peptide was incorporated into the vesicles, the desired amount of peptide in methanol was added to the lipid mixture at this time. Solvent was removed by rotary evaporation at 70°C using a Büchi R-3000 rotary evaporator (Flawil, Switzerland). The lipid film was placed under vacuum for at least 4 hours then hydrated at room temperature by vortexing for at least 2 minutes with buffer

containing 20 mM MOPS (3-(N-morpholino)propane-sulfonic acid), pH 7.5, 0.1 mM EGTA, 0.02% $NaNH_3$, and 100 mM KCl. Vesicles containing BSM were hydrated with buffer at 70°C. The vesicle suspension was then extruded 10 times through two stacked Nuclepore polycarbonate filters with a pore size of 0.1 μm, using a high-pressure extruder (Lipex Biomembranes Inc., Vancouver, British Columbia, Canada) at room temperature for POPC vesicles, and at 70 ºC for SM containing mixtures, to ensure conversion of all multilamellar vesicles to unilamellar vesicles of uniform size. Lipid concentrations for vesicles and lipid stocks were determined using a Bartlett phosphate assay (15), modified as described by Pokorny et al. (16). In the Bartlett assay, formation of a phosphomolybdate complex occurs through reaction of ammonium molybdate and ascorbic acid with inorganic phosphate derived from the lipid phosphate groups. This complex absorbs at 580 nm. A standard curve, performed in triplicate, was prepared from absorbance values of phosphate solution with concentrations from 0 to 316 nmoles. Lipid concentrations were calculated using a linear fit.

Synthesis of NBD-POPE

Molecular sieves (Sigma-Aldrich, St. Louis, MO) were dried for five hours at 80°C. Organic solvents $CHCl_3$ and methanol MeOH were poured over the sieves and allowed to dry overnight. POPE solution in $CHCl_3$ was dried using a rotary evaporator to produce a thin lipid film. The film was dissolved in approximately 0.7 mL of dry $CHCl_3$. Approximately 0.5 mg of NBD-Cl was reacted in a probe/lipid ratio of 1:1.1 with POPE. Solid NBD-Cl was dissolved in as little dry 1:1 $CHCl_3$/MeOH as possible (approximately 0.7 mL). Crushed potassium carbonate (K_2CO_3) which had been dried for 48 hours at 80°C, was added to the dried POPE solution in a 1:1.1 lipid/salt ratio. The NBD-Cl was added to the POPE/K_2CO_3 solution drop-wise while stirring.

The reaction mixture was allowed to stir in the dark and reaction progress was monitored by TLC using a solvent system of 2:1 dichloromethane (CH_2Cl_2)/MeOH for NBD. NBD was identified using UV light and the phosphorous-containing POPE was identified using the Zinzade reagent. The reaction was complete after 6.5hrs.

Purification was performed on a preparatory TLC plate (Uniplate® (20 x 20 cm, 1000 microns)) using 4:1 CH_2Cl_2/MeOH. Two product bands (product A and product B) were removed from the preparatory plate and each product was eluted from the silica using 4:1 CH_2Cl_2/MeOH and a sintered glass funnel. Both product bands were analyzed and compared with NBD-POPE stock by TLC using 4:1 CH_2Cl_2/MeOH and product A was found to be pure NBD-POPE. Solvent was removed by rotary evaporation at 50°C and the NBD-POPE product was dissolved in a minimal amount of dry $CHCL_3$ and stored at -30°C. Probe concentration was determined using a CARY 1E UV-Visible Spectrophotometer (Varian, Australia). NBD-POPE has a molar absorptivity of 21,000 M^{-1} cm^{-1} at 463 nm in MeOH. The structure of NBD-POPE is shown in Figure 3.

Synthesis of MB-POPE

Molecular sieves were dried for five hours at 80°C. Organic solvents $CHCl_3$ and dimethylformamide (DMF) were poured over the sieves and allowed to dry overnight. POPE solution in $CHCl_3$ was dried using a rotary evaporator to produce a thin lipid film. The film was dissolved in approximately 0.7 mL of dry $CHCl_3$. Approximately 0.5 mg of MB-SE was reacted in a probe/lipid ratio of 1:1.1 with POPE. Solid MB-SE was dissolved in as little dry DMF as possible (approximately 0.3 mL). Crushed potassium carbonate (K_2CO_3) which had been dried for 48 hours at 80°C, was added to the dried POPE solution in a 1:1.1 lipid/salt ratio. The MB-SE solution was added to the POPE/K_2CO_3 mixture drop-wise while stirring. The reaction

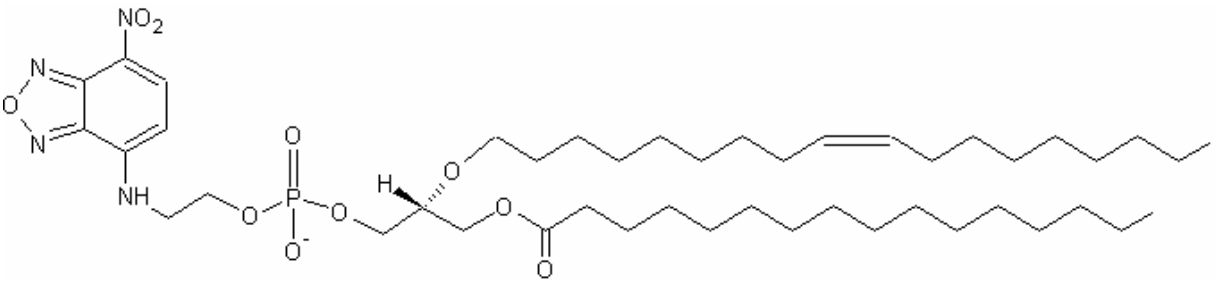

Figure 3. Structure of NBD-POPE at pH 7.50.

mixture was allowed to stir in the dark and reaction progress was monitored by TLC using a solvent system of 2:1 dichloromethane (CH_2Cl_2)/MeOH. MB was identified using UV light and the phosphorous-containing POPE was identified using the Zinzade reagent. The reaction was complete after 2hrs.

Purification was performed on a preparatory TLC plate using 3.5:1 CH_2Cl_2/MeOH. Two product bands (product A and product B) were removed from the preparatory plate and each product was eluted from the silica using 2:1 CH_2Cl_2/MeOH and a scintered funnel. Both product bands were analyzed and compared with MB-POPE stock by TLC using 65:25:4 CH_2Cl_2/MeOH/H_2O and product A was found to be pure MB-POPE. Solvent was removed by rotary evaporation at 50°C. The MB-POPE product was dissolved in a minimal amount of $CHCL_3$ and stored at -30°C. Probe concentration was determined using a CARY 1E UV-Visible Spectrophotometer. MB-POPE has a molar absorptivity of 24,000 M^{-1} cm^{-1} at 368 nm in basic MeOH. The structure of MB-POPE is shown in Figure 4.

Fluorescence Spectroscopy Experiments

Fluorescence measurements were preformed in a SLM-Aminco 8100 spectrofluorometer (Urbana, IL). For tryptophan emission experiments, Trp was excited at 270 nm and emission wavelength was scanned from 300 nm to 500 nm. For FRET experiments with the donor/acceptor pair MB-POPE and NBD-POPE, MB-POPE was excited at 367 nm and emission wavelength was scanned from 400 to 600 nm. The slit widths were 2 nm (excitation) and 8 nm (emission) for all measurements. Energy transfer efficiency from MB-POPE to NBD-POPE was calculated using Equation 1 (5)

$$E_t = \frac{6.66 p_r^{2.33}}{1 + 6.66 p_r^{2.33}} - 0.048 \qquad (1)$$

where p_r is the fluorescence peak ratio of NBD emission at 524 nm to MB emission at 460 nm.

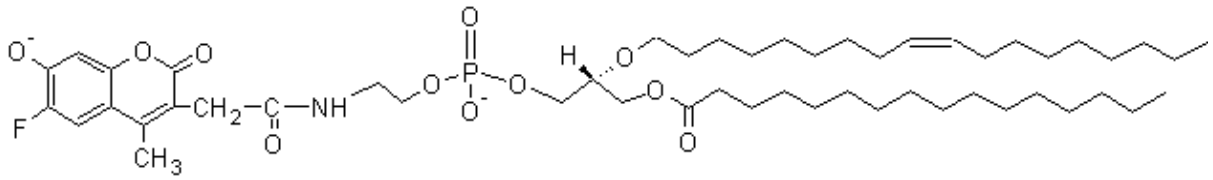

Figure 4. Structure of MB-POPE at pH 7.50.

Monte Carlo Simulations

Monte Carlo simulations were performed on a Linux workstation with in-house FORTRAN code programs using the NAG f95 compiler (Numerical Algorithms Groups, Oxford, UK). In the simulations, the phospholipid bilayer was represented by two superimposed triangular lattices each containing 100 X 100 sites with skew-periodic boundary conditions. Each site on the lattice represents a lipid molecule (POPS, POPC, or Chol). A fixed number of proteins was used in each simulation. Each protein, when bound to the bilayer is represented by a 19-site hexagon on the lattice. This hexagon is divided into an inner 7-site core hexagon and a 12-site border. The 7-site core is responsible for general binding to the membrane, with an association constant K_0=exp(-$\Delta G_0/RT$), while the 12-site border preferentially binds to negatively charged lipids (PS) with a favorable binding free energy of ω_p for each site underneath the protein border. Some implement a preferential protein-protein interaction parameter (ω_a). Lattice lipids are either zwitterionic (PC) or negatively charged (PS) or in some systems cholesterol. In the simulations, proteins are allowed to associate with and dissociate from the lattice surface. Protein diffusion on the lattice surface (movement of a protein center from one site to another) is also allowed; however protein-protein overlap is not allowed. Lipids are allowed to diffuse within the bilayer as well as flip between the inner and outer layer of the lattice.

The Metropolis algorithm (17) was applied in the simulations to allow for either the acceptance or rejection of moves. Moves are accepted if the change in free energy associated with the move is less than 0, or if the probability, p=exp(-$\Delta G/RT$), of the move is greater than or equal to a random number (*Ran#* between 0 and 1). The change in free energy is calculated by

$$\Delta G = \omega_{ab}\Delta n_{ab} + \Delta P \Delta G_O + G_{Bind} \qquad (2)$$

where $\omega_{ab} = \varepsilon_{ab} - (\varepsilon_{aa} + \varepsilon_{bb})$ is the unlike nearest-neighbor interaction parameter, Δn_{ab} is the change in the number of unlike neighbors, ΔP is the change in the number of bound proteins, and $G_{Bind} = \omega_p N + \omega_a M$ where ω_p is the preferential protein-lipid interaction, N is the number of PS lipids under the protein, ω_a is the protein-protein interaction, and M is the number of neighboring proteins.

The algorithm is as follows. First, a designated number of diffusion Monte Carlo cycles (mcc) are performed to achieve equilibrium with respect to lipid distribution on the bilayer. Each lipid cycle consists of lipid diffusion with a standard Kawasaki step (18). Next, a series of total mcc are performed in order to achieve equilibrium with respect to protein distribution. These cycles consist of protein binding, protein diffusion, and lipid diffusion. Each protein cycle is as follows. First a random site on the lattice is picked. If there is a protein bound to this position, the program decides randomly between protein diffusion and protein desorption. If protein desorption is chosen, the probability of dissociation is calculated using the following equation

$$p_{off} = \frac{(k_{on} K_a)}{(1 + k_{on} K_a)} \tag{3}$$

where k_{on} is the on rate constant and K_a is given by Equation 4

$$K_a = \exp\left(\frac{G_{off} + G_{bind}}{RT} \right) \tag{4}$$

The protein will dissociate from the lattice if p_{off} > RAN#. If protein diffusion is chosen, a

neighboring site on the lattice is chosen at random and the protein is moved to that site. The move is either accepted or rejected according to the previously described Metropolis algorithm. If no protein is bound on the chosen site, then the program will try to bind the protein. The binding probability is calculated using Equation 5

$$p_{on} = \frac{k_{on}[P]}{1+(k_{on}[P])} \tag{5}$$

where [P] is the concentration of protein in solution.

Monte Carlo Parameters. A quantitative study of annexin binding to the lipid bilayer was performed using Monte Carlo computer simulations. Before this study could be performed, simulations were conducted to determine estimates of the annexin binding free energy to PC (G_{off}) and the interaction between annexin and PS (ω_P). To obtain these values, the apparent dissociation constant (K_{app}) for systems containing 50 annexin proteins was calculated using Equation 6.

$$K_{app} = K_L \frac{(1+K_1[Ca^{2+}])^n}{(1+K_0[Ca^{2+}])^n} \tag{6}$$

In this equation, K_L is the lipid affinity in the absence of Ca^{2+}, K_0 is the binding constant for Ca^{2+}, K_1 is the binding constant for Ca^{2+} in the presence of lipid, [Ca^{2+}] is the calcium concentration in the system, and n is the maximum number of Ca^{2+} ions that can be bound per annexin (n = 9) (12). The lipid affinity in the absence of Ca^{2+} (K_L) depends on the mole fraction of PS (X_{PS}) in the system. This dependence is described by

$$K_L = A_o \exp\left(K_{PS} X_{PS}\right) \tag{7}$$

where A_0 is the binding constant to pure PC vesicles, X_{PS} is the mole fraction of PS in the system, and K_{PS} is a constant describing the dependence on PS content. Previous experimental research has determined these parameters for annexin A5 (12). The parameters for A5 are $K_0 = 6.0 \times 10^4$ M^{-1}, $K_1 = 1.7 \times 10^5$ M^{-1}, $A_0 = 6.3 \times 10^2$ M^{-1}, and $K_{ps} = 8.05$. Using these constants, estimates of the experimental K_{app} were calculated for systems containing 100% PC and 50 A5 proteins. Within the program, G_{off} was varied until the theoretical Monte Carlo K_{app} matched the experimental K_{app}. Monte Carlo K_{app} was calculated for each system using Equation 8

$$K_{app} = \frac{\left[Anx(POPC)\right]}{\left[Anx\right]\left[POPC\right]} \tag{8}$$

where [Anx(POPC)] is the concentration of annexin bound to PC, [Anx] is the total annexin concentration and [POPC] is the total POPC concentration. This was performed for systems with varying calcium concentrations. For simulations of systems containing 95:5 PC/PS and 50 annexin proteins, ω_p was varied until the Monte Carlo K_{app} matched the experimental K_{app}. This was also performed at various calcium concentrations.

The protein binding free energy to PC (G_{off}) and the interaction between the protein and PS (ω_p) were determined for annexin A5 using Monte Carlo computer simulations. The G_{off} and ω_p for C2 simulations were obtained from previous experimental and Monte Carlo simulations (4). Monte Carlo determinations for protein binding free energy and protein-PS interactions for A5 and C2 are listed in Table 1. Estimates for unlike lipid interactions between PS and PC (ω_{SC}), PS

and Chol (ω_{DS}), and Chol and PC (ω_{DC}) are listed in Table 2 (6). The estimate for the unlike lipid interaction between PS and PC (ω_{SC}= +240 cal/mol) was obtained from the work of Hinderliter et al (4). This estimate was obtained by matching experimental binding data with simulated data. The value for the interaction between PC and Chol (ω_{DC}= +200 kcal/mol) was obtained from work done by Frazier et al. (5). The estimate for ω_{DS} was approximated on the basis that unfavorable unlike lipid interactions are typically on the order of 200-300 cal/mol (19).

All simulations consisted of approximately 500,000 equilibration cycles followed by 1,000,000 total mcc to ensure complete system equilibration. For each simulation the number of bound proteins, distribution of protein and lipid domains, and size of protein and lipid domains were monitored. PS domains are defined as a cluster of at least two PS lipids. In some cases, the distribution of lipid species between the inner and outer monolayer was also monitored.

Table 1. Protein binding free energy to PC (G_{off}) and protein-PS interaction (ω_P) for annexin A5 and the C2 protein motif in the presence and absence of Ca^{2+}.

Protein	**[Ca^{2+}] (μM)**	**G_{off} (kcal/mol)**	**ω_p (cal/mol)**
Annexin A5	0	-3.8	-215
	20	-7.6	-162
	100	-8.9	-156
C2	0	-5.0	-1000

Table 2. Lipid-lipid interactions between PS and PC (ω_{sc}), Chol and PC (ω_{dc}), and Chol and PS (ω_{ds}) lipids.

Bilayer System	ω_{sc} **(cal/mol)**	ω_{dc} **(cal/mol)**	ω_{ds} **(cal/mol)**
PC/PS	+240	0	0
PC/PS/Chol	+240	+200	-250

RESULTS

Monte Carlo Studies

PC/PS Bilayers and Lipid Domains. Monte Carlo computer simulations were performed to investigate the ability of annexin A5 to induce PS domain formation upon binding to PC/PS bilayers. These simulations were performed for systems consisting of 80:20, 60:40, and 20:80 PC/PS, each in the presence and absence of calcium. For each lipid composition, the total number of proteins was increased from 0 to 200 and the average domain size for PS lipids and proteins was recorded. To account for the protein-PS interaction specific to A5, the ω_p parameter was -156 cal/mol and -162 cal/mol to account for the absence and presence of 100 μM Ca^{2+} respectively (Table 1). The values for these interactions were obtained by determining Monte Carlo K_{app} for binding in the presence and absence of Ca^{2+} as described in the methods section. Also, the unlike lipid interaction between PS and PC (ω_{sc}) was kept at +240 cal/mol for each simulation (4).

The change in PS distribution as A5 concentration was increased from 0 to 200 proteins was monitored in the presence and absence of 100 μM Ca^{2+}. Simulations of A5 binding to 80:20, 60:40, 40:60, and 20:80 PC/PS show that for all mixtures, the average PS domain size is the same with (gray) and without (black) 100 μM Ca^{2+} for all A5 concentrations (0 to 200 proteins) (Figure 5 A, B, C, D). Also, in the absence of Ca^{2+}, at low protein concentrations, only approximately 25% of the A5 proteins would bind to the lattice. At the highest A5 concentration (200 proteins) only 75% of all proteins were bound to the lattice. Addition of Ca^{2+} to these systems does not greatly enhance the effect of A5 on lipid domain formation. However, for all simulations 100% of the total protein content bound to the lattice. This demonstrates that while binding of A5 depends on the presence of Ca^{2+}, this protein binding does not affect lipid distribution. The PS distribution plots indicate that PS domain size does increase from systems

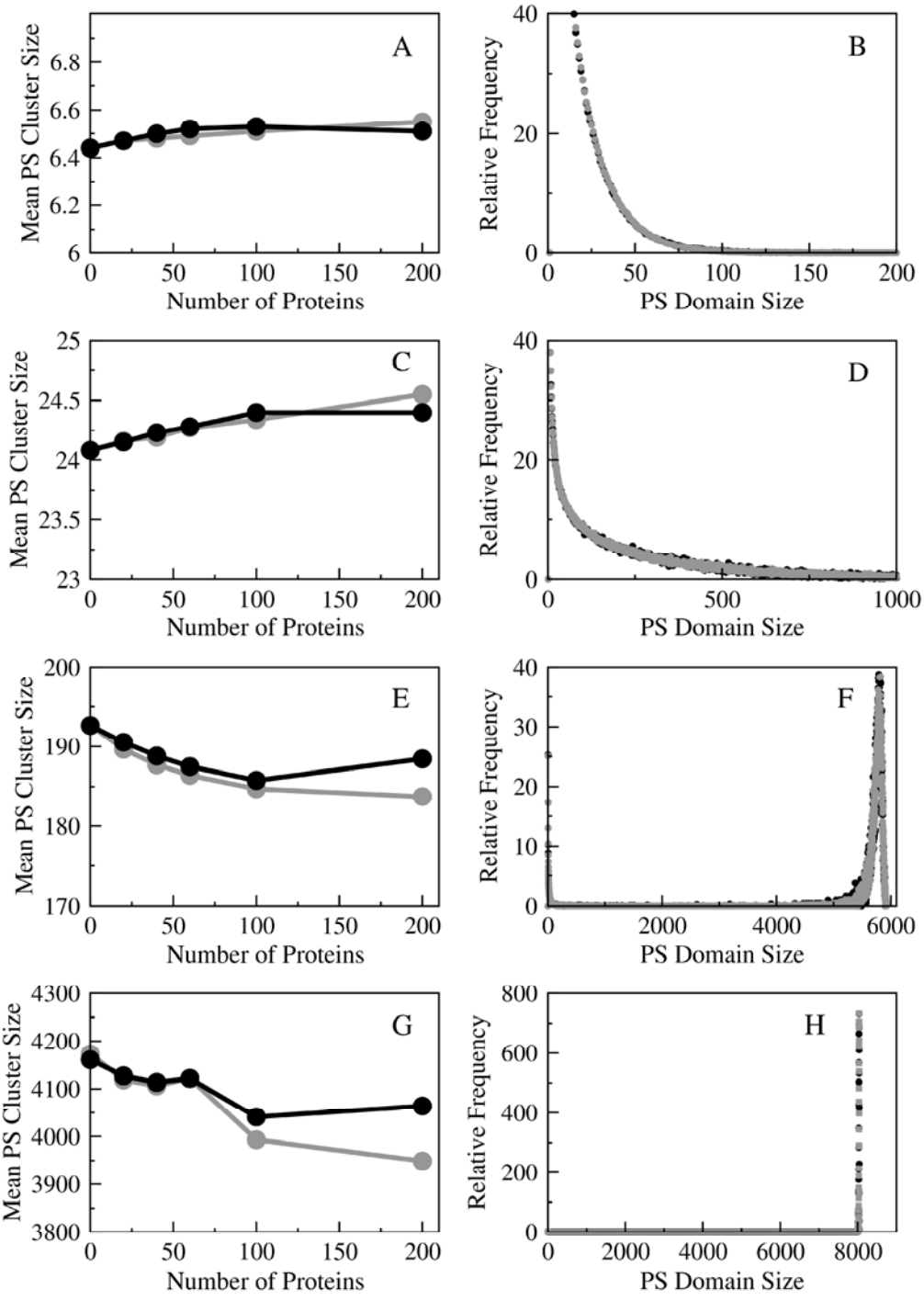

Figure 5. Mean PS cluster size and PS distribution upon addition of A5 (0 to 200 proteins) to PS/PC mixtures in the presence (gray) and absence (black) of 100 μM Ca^{2+}. Results are for mixtures containing 20:80 PC/PS (A, B), 40:60 PC/PS (C, D), 60:40 PC/PS (E, F), and 80:20 PC/PS (G, H). PS distribution plots are for simulations with 100 A5**.** For all protein concentrations, 100% and 25-75% A5 was bound to the lattice with and without 100 μM Ca^{2+} respectively.

containing 20 % PS to systems containing 80 % PS; however, this trend is only a result of increasing PS content within the vesicles (Figure 5 B, D, F, H).

Monte Carlo simulations were also performed including a favorable protein-protein interaction (ω_a). A favorable protein-protein interaction introduces the possible protein-clustering ability of A5 upon binding to PC/PS systems. For simulations with this favorable interaction, the value for protein-protein interactions was chosen to be ω_a= -2.0 kcal/mol. For simulations not including this favorable protein-protein interaction, ω_a was set to 0 kcal/mol.

Simulations of A5 binding were performed in the presence of 20 μM Ca^{2+} for lipid compositions of 20, 30, 40, and 60 % PS. Data was collected in the presence of 20 to 80 proteins, with ω_a= 0 kcal/mol (black) and ω_a= -2 kcal/mol (gray) (Figure 6). Results from these simulations show that making the protein-protein interaction favorable (ω_a= -2 kcal/mol) very slightly magnifies the extent of lipid demixing upon binding of A5 for all PC/PS systems. Simulations of A5 on binary systems of PC/PS show little increase in PS cluster size when ω_a= -2.0 kcal/mol when compared to A5 binding when ω_a= 0 kcal/mol (Figure 6). Specifically, for A5 on 80:20 PS/PC, the average PS domain size only increases from approximately 6.5 to 6.7 lipids at high protein concentration when the favorable protein-protein interaction is included in the simulations (Figure 6 A, B). Bilayer and protein snapshots for binding of 80 A5 with ω_a= -2.0 kcal/mol shows that while A5 clusters when bound to the lattice, this clustering does not induce the formation of PS domains corresponding to the protein clusters (Figure 7 C, D).

Similar simulations were performed to monitor the effect of a favorable protein-protein interaction (ω_a= -2.0 kcal/mol) to PC/PS systems in the presence of the C2 protein motif. Similarly to the annexins, C2 binds to negatively charged lipids in a Ca^{2+}- dependent manner. It has been shown through experimental and computational work that binding of C2 to PC/PS mixtures induces the formation of lipid domains (4). Since it is believed that the ability of

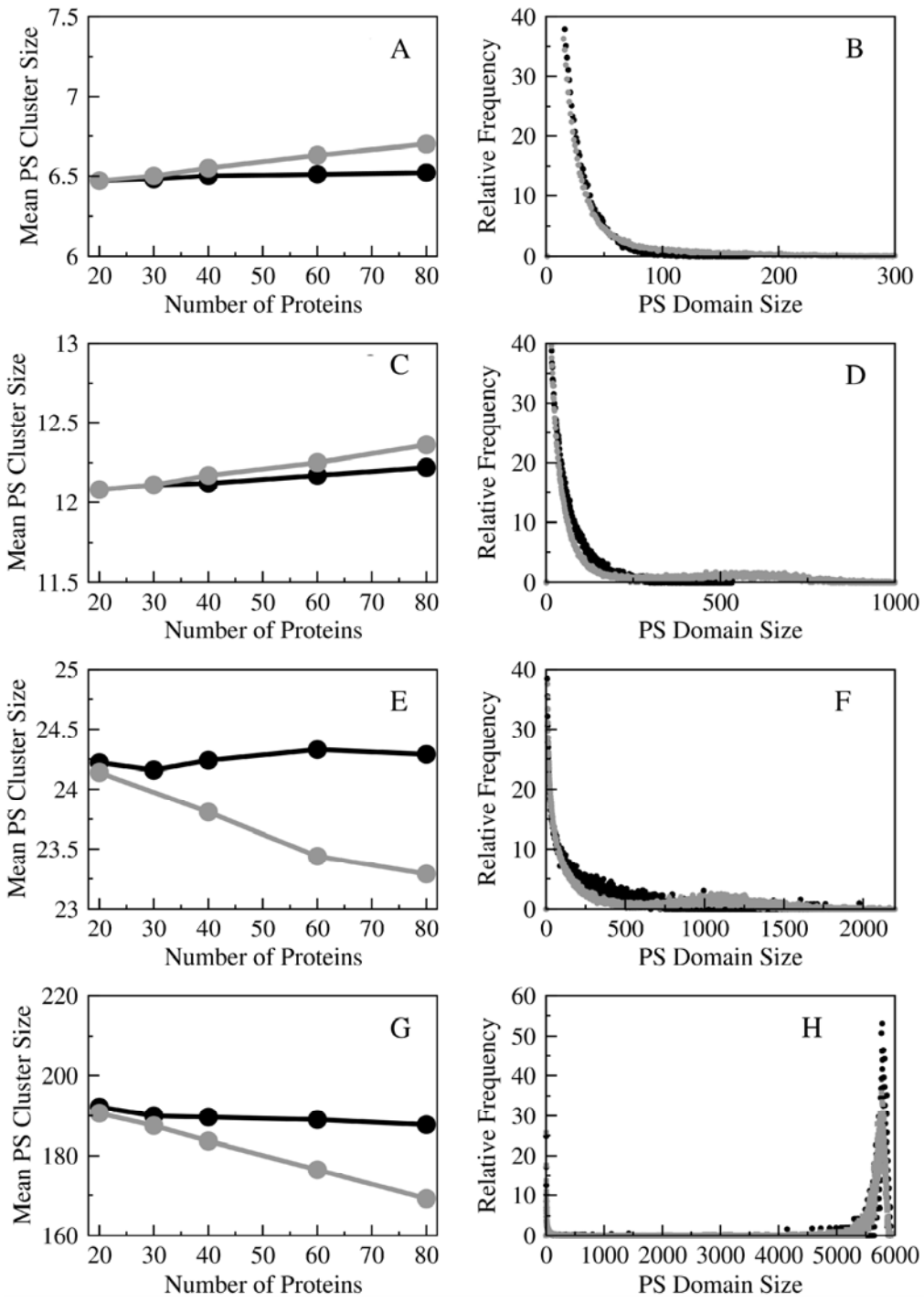

Figure 6. Mean PS cluster size and PS distribution upon addition of A5 (20 to 80 proteins) with protein-protein interaction ω_a= 0 kcal/mol (black) and ω_a= -2.0 kcal/mol (gray). Results are shown for mixtures containing 20:80 PC/PS (A, B), 30:70 PC/PS (C, D), 40:60 PC/PS (E, F), and 60:40 PC/PS (G, H). PS distribution is representative of binding of 60 A5. For all simulations, 100% of the total A5 concentration was bound to the lattice.

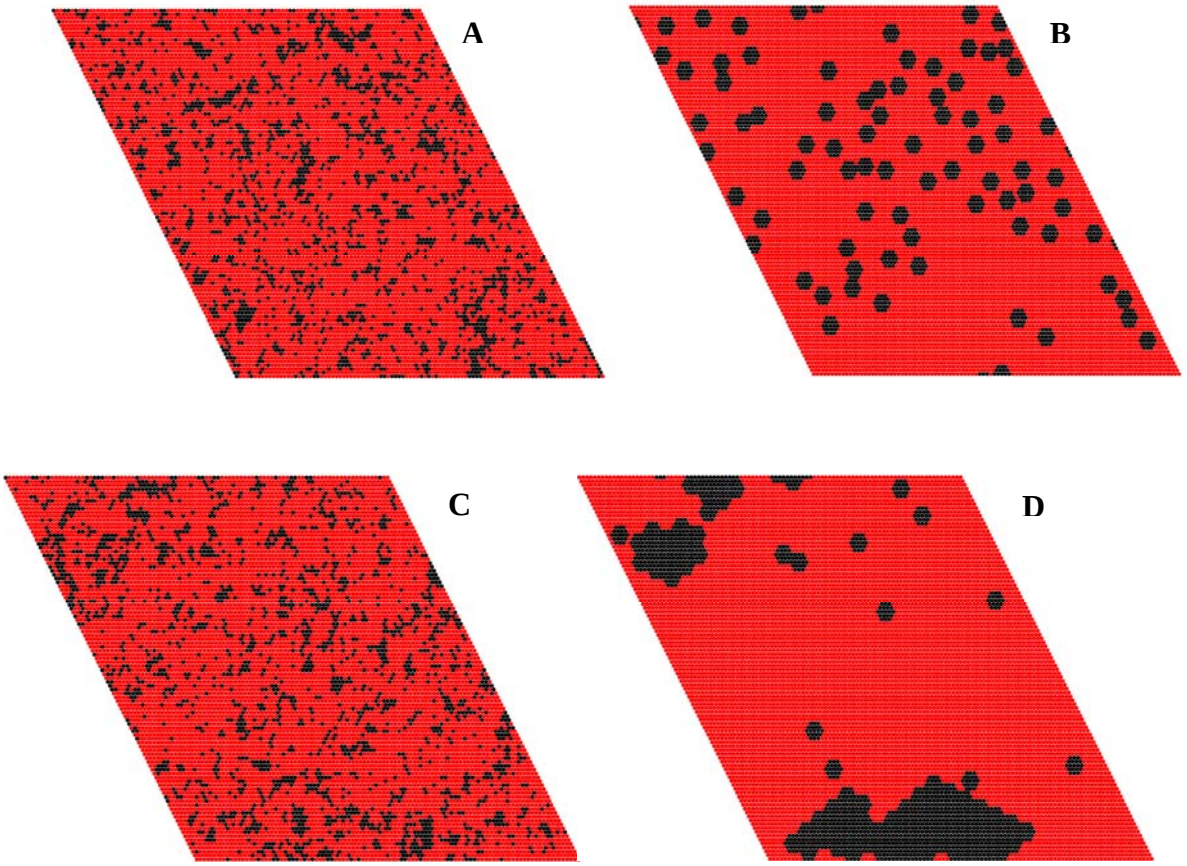

FIGURE 7. Bilayer and protein snapshots for 80:20 PC/PS with protein-protein interaction of 0 kcal/mol (A, B) and -2.0 kcal/mol (C, D) in the presence of 80 A5 proteins. In the protein snapshot (right) the large black hexagons represent individual A5 proteins. In the bilayer snapshot (left), PS molecules are black, and PC molecules are red.

protein binding to induce lipid domain formation depends on the sum of all thermodynamic interactions involved, creating a favorable protein-protein interaction for C2would be expected to enhance its lipid clustering ability. All simulations were completed for systems containing 80:20 PC/PS (Table 2).

Results in Figure 8 (top) indicate that binding of C2 induces PS domain formation with a maximum average PS domain size of approximately 10 lipids in the presence of 80 proteins (black). The presence of a favorable protein-protein interaction for C2 greatly enhances the extent of lipid demixing upon binding when protein concentration is high (80 to 100 proteins) with an average PS domain size of approximately 16 lipids in the presence of 100 proteins (Figure 8, gray). However, at lower protein concentrations (20 to 60 proteins) the ability of C2 to induce PS domains remains unaffected. Bilayer and protein snapshots for binding of 80 C2 with ω_a= -2.0 kcal/mol show that when bound to the lattice, C2 forms large protein clusters on the lattice surface with large PS domains directly corresponding to protein clusters (Figure 9 C, D). Without the favorable protein-protein interaction, C2 does not form large clusters which results in smaller PS domains (Figure 9 A, B). This is further illustrated by the PS distribution in Figure 8 (bottom), which shows the presence of many large PS domains (over 1000 PS molecues) when ω_a= -2.0 kcal/mol (gray).

PC/PS/Chol Bilayers and Lipid Domains. Monte Carlo computer simulations were performed to monitor the effect of the addition of cholesterol to the previously described PC/PS lattice system. It has been shown that cholesterol can form a condensed complex with PS (21). Annexin, as well as the C2 motif, are known to associate with negatively charged lipids, such as PS, and are believed not to associate with cholesterol. Therefore, any changes in lipid distribution induced by the proteins should arise from interactions between cholesterol and PS lipids and not with the associated proteins. The simulations were performed on systems

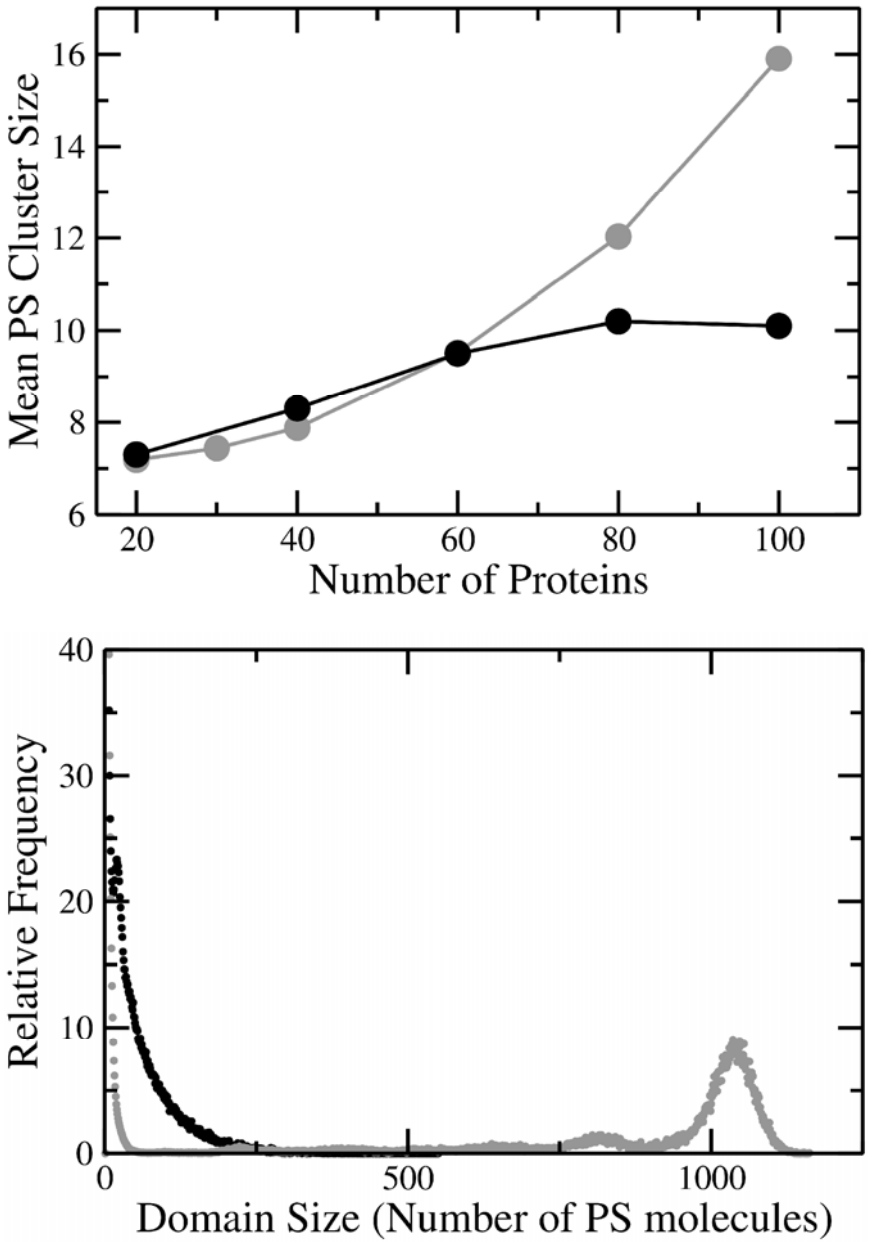

Figure 8. Mean PS cluster size upon addition of C2 (20 to 100 proteins) to 80:20 PC/PS with (gray) and without (black) protein-protein interaction (ω_a= -2.0 kcal/mol) (top). PS distribution for 80:20 PC/PS and 80 C2 (bottom) with protein-protein interaction ω_a = 0 kcal/mol (black) and ω_a= -2.0 kcal/mol (gray). For all simulations, 100% of the total C2 concentration was bound to the lattice.

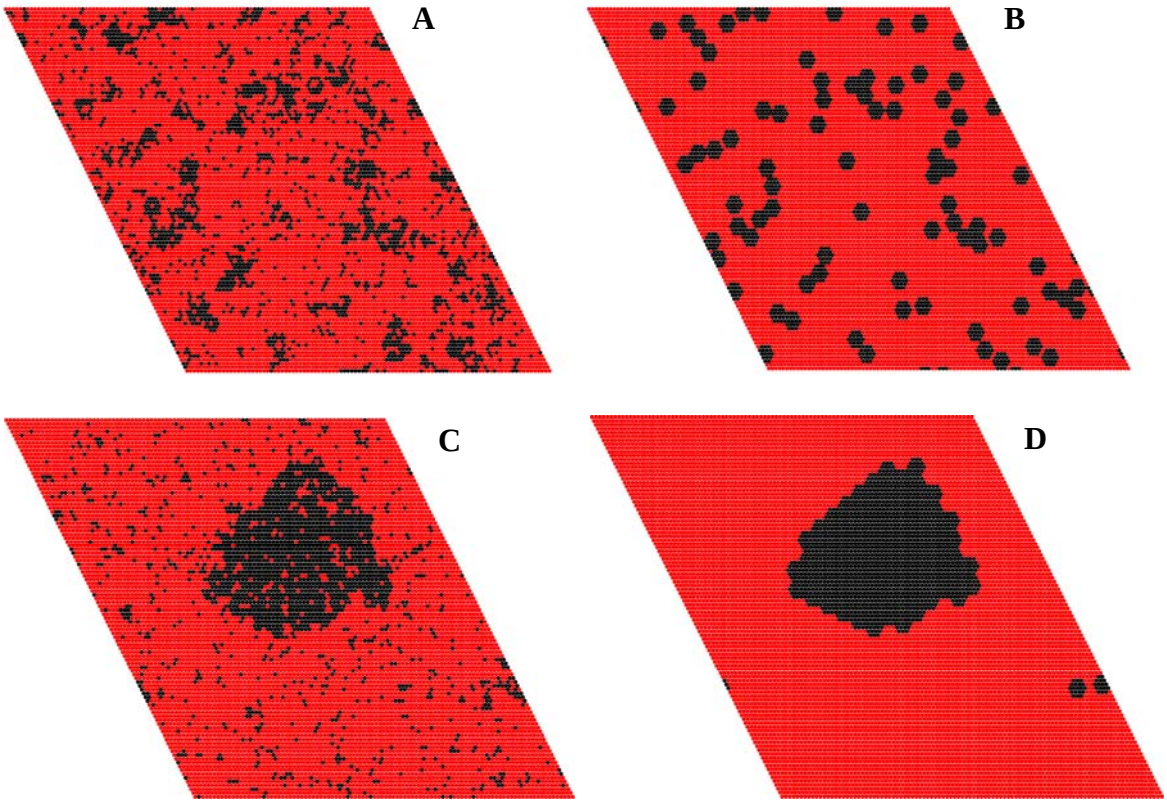

FIGURE 9. Bilayer and protein snapshots for 80:20 PC/PS with protein-protein interaction of 0 kcal/mol (A, B) and -2.0 kcal/mol (C, D) in the presence of 80 C2 proteins. In the protein snapshots the large black hexagons represent individual C2 proteins. In the bilayer snapshots, PS molecules are black, and PC molecules are red.

containing PS, PC and Chol with a fixed 20 mol % PC and 100 proteins in the presence of Ca^{2+}. To account for the favorable PS-Chol interaction, additional lipid-lipid interactions were incorporated into the MC simulations (Table 2). An actual measure for the interaction between Chol and PS (ω_{DS}) does not exist; therefore an estimate had to be made. Typically, unlike lipid interactions are a few hundred calories per mole, and the value for ω_{DS} was chosen to be -250 cal/mol to indicate a favorable interaction between the lipid species. Also, the Chol-PC interaction (ω_{DC}) was +200 cal/mol (5) and the PS-PC interaction (ω_{SC}) was +240 cal/mol.cal/mol. The total Chol concentration was varied between 0 to 40 mol %.

Monte Carlo simulations were performed in the presence and absence of 100 A5 proteins. Simulations were also performed with the favorable protein-protein interaction parameter included (ω_a= -2.0 kcal/mol). For each simulation, the number of proteins bound, distribution of proteins and lipid domains, and the size of lipid domains was monitored. When A5 is mixed with PC/PS/Chol bilayers, a maximum average PS domain size is observed for systems containing 10 % Chol in the absence and presence of A5, as well as when the favorable protein-protein interaction was set to -2 kcal/mol (Figure 10). This maximum domain size increases from 9 lipids when ω_a= 0 kcal/mol (Figure 10, green) to 11 lipids when ω_a= -2.0 kcal/mol (Figure 10, purple). Therefore, PS domain size depends not only on protein binding, but also bilayer composition. Simulation snapshots for 70:20:10 PC/PS/Chol mixtures with the protein-protein interaction of 0 kcal/mol and -2.0 kcal/mol (Figure 11) illustrate how a favorable protein-protein interaction greatly enhances the extent of lipid demixing upon binding of A5. When ω_a= 0 kcal/mol (Figure 11 A, B) A5 does not cluster on the lattice surface and only small to medium sized domains are observed on the bilayer. When ω_a= -2.0 kcal/mol, large A5 clusters are present on the lattice surface, and large PS domains correspond to these clusters (Figure 11 C, D).

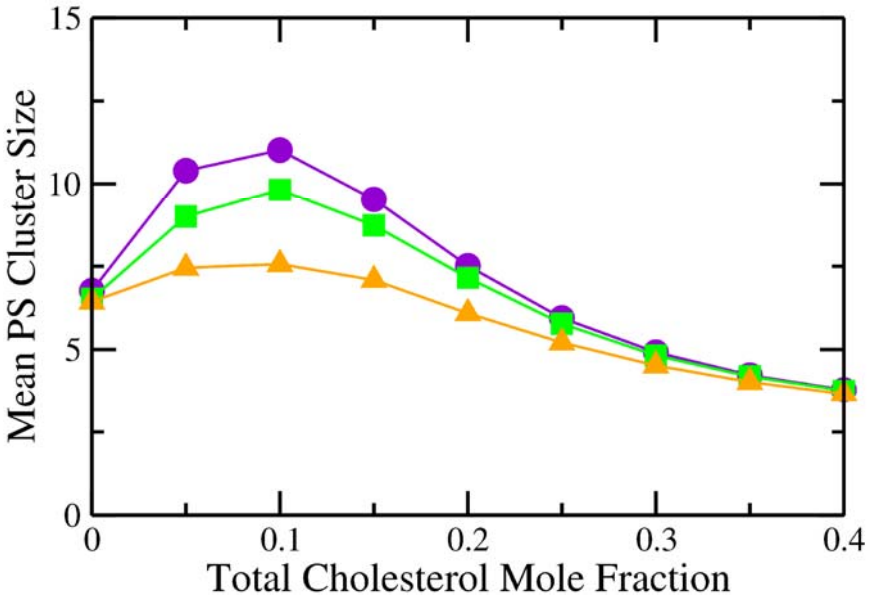

FIGURE 10. Mean PS domain size for PC/PS/Chol systems in presence of 100 A5 with protein-protein interaction ω_a= 0 kcal/mol (green square), ω_a= -2.0 kcal/mol (purple circle), and without protein (orange triangle). All simulations consisted of at least 800,000 monte carlo cycles and 400,000 equilibration cycles.

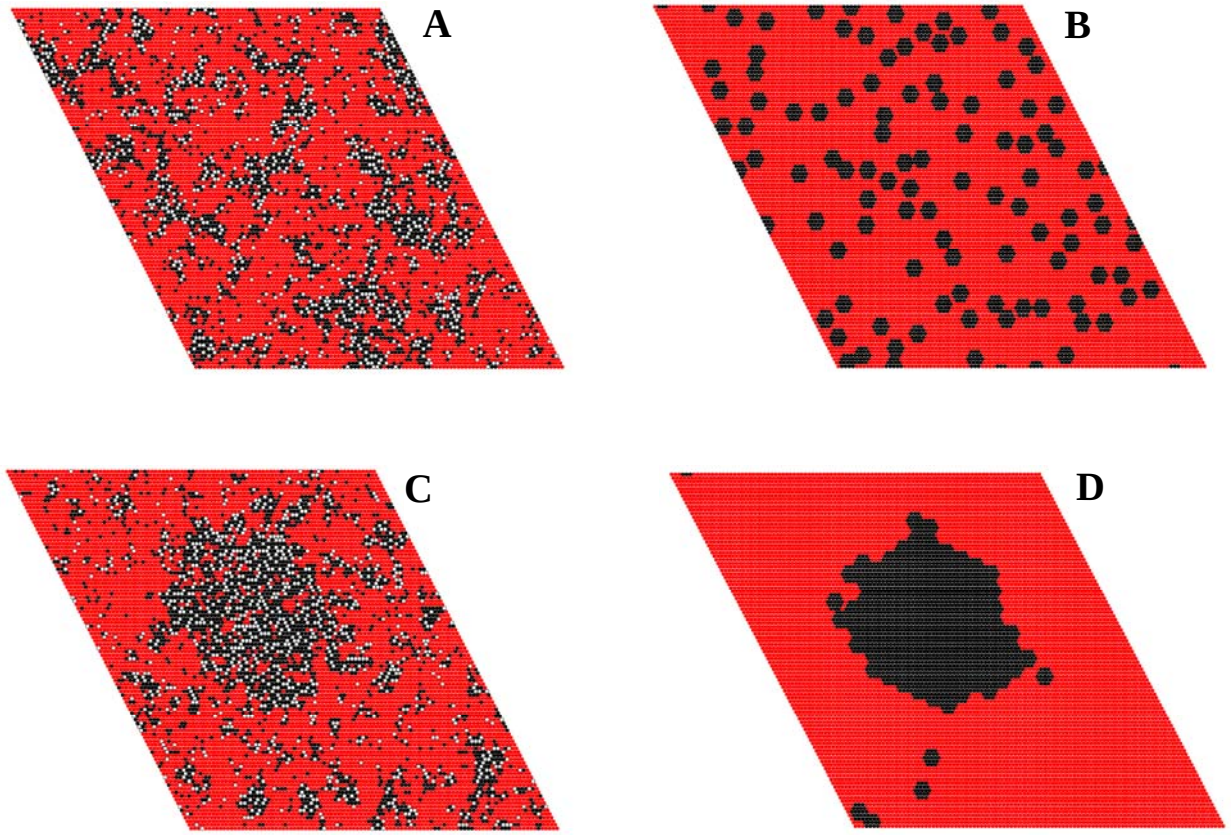

Figure 11. Bilayer and protein snapshots for 70:20:10 PC/PS/Chol with protein-protein interaction of 0 kcal/mol (A,B) and -2.0 kcal/mol (C,D) in the presence of 100 A5 proteins. In the protein snapshots (B, D) the large black hexagons represent individual C2 proteins. In the bilayer snapshots (A, C) PS molecules are black, Chol molecules are white, and PC molecules are red.

The distribution of PS molecules for mixtures containing 10 mol % Chol was plotted for all simulations and is shown in Figure 12. These plots indicate that a many large PS domains do not appear until a protein-protein interaction of -2.0 kcal/mol is included in the simulation parameters. Specifically, PS distribution in Figure 12 for ω_a= 0 kcal/mol (green) shows the presence of many small domains with only very few domains reaching a size of 500 lipids. However, when ω_a= -2.0 kcal/mol (purple) this distribution shifts to show the presence of many large PS domains of approximately 950 lipids. It is important to note that while the average PS domain size (Figure 10) only seems to slightly increase from 9.8 to 11.0 lipids when ω_a is changed from 0 to -2.0 kcal/mol, both the lattice snapshots (Figure 11) and PS distribution plots (Figure 12) indicate that a much larger increase in PS domain size occurs upon binding of C2 with ω_a= -2.0 kcal/mol. Therefore, it is critical to monitor not only the average lipid domain size, but lipid distribution and lattice snapshots for each simulation.

Similar simulations were performed to monitor binding of the C2 protein motif to PC/PS/Chol mixtures. C2 binding to PC/PS mixtures has already demonstrated the ability of C2 to induce the formation of lipid domains in the presence of Ca^{2+} (Figure 8). Binding of C2 to mixtures containing PC/PS/Chol should induce much larger PS domains than A5 because of its much more favorable protein-PS interaction coupled with the favorable PS-Chol interaction. As shown in Figure 13, addition of C2 to such mixtures induces the formation of very large PS domains (green). The size of these domains depends on the total Chol mole fraction within the bilayer. When 10% Chol is present, a maximum average PS domain size of 23 lipids is observed. This shows that the size of the PS domains in PC/PS/Chol mixtures depends on both the protein bound and the bilayer composition. For simulations of C2 binding with ω_a= 0 kcal/mol, the trend of average PS domain size is similar to that of A5, with the largest average domain size of 23 PS lipids again at 10 % Chol. A favorable protein-protein interaction of

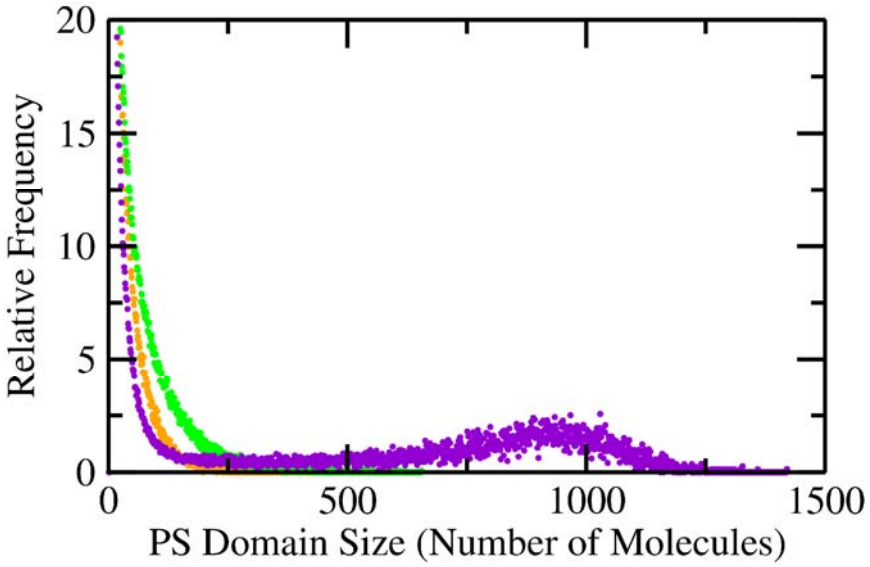

Figure 12. PS lipid distribution for 70:20:10 PC/PS/Chol in the presence of 100 A5 with protein-protein interaction ω_a= 0 kcal/mol (green), 2.0 kcal/mol (purple), and in the absence of protein (orange).

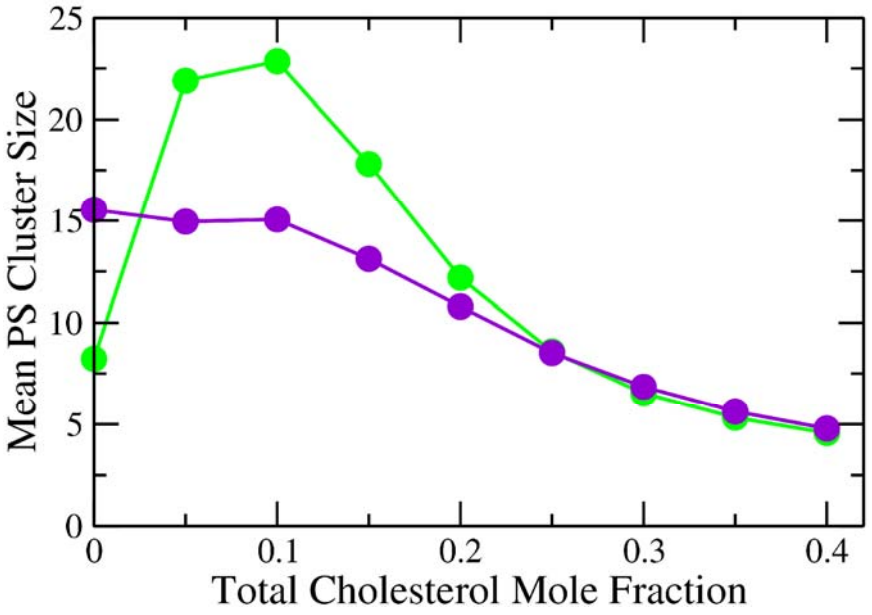

Figure 13. Mean PS domain size for PC/PS/Chol systems in presence of 100 C2 with ω_a= 0 kcal/mol (green) and ω_a= -2.0 kcal/mol (purple). All simulations consisted of at least 400,000 equilibration cycles followed by at least 800,000 monte carlo cycles.

kcal/mol would be expected to further increase the average PS domain size upon binding of C2 because of the overall increase in thermodynamically favorable interactions. However, results in Figure 13 show that the average PS domain size decreases when ω_a= -2.0 kcal/mol (purple), with a maximum domain size of only 15 lipids.

Further investigation of PS distribution (Figure 14) for all mixtures with ω_a= 0 kcal/mol (black) and -2.0 kcal/mol (gray) indicates that addition of a favorable protein-protein interaction of -2.0 kcal/mol greatly alters PS distribution, resulting in a bimodal distribution of PS domain size when ω_a= -2.0 kcal/mol. This is most apparent for mixtures containing 0 to 20 mol % Chol. For these mixtures, PS distribution plots contain a single large peak for lipid domains containing more than 1000 PS lipids as well as many domains containing only a few PS lipids. Simulations performed with ω_a= 0 kcal/mol show a broad distribution of PS domains for these mixtures with many small PS domains and relatively the same amount of medium and large PS domains.

Lattice and protein snapshots for simulations with ω_a= 0 kcal/mol and -2.0 kcal/mol and 10 mol % Chol further illustrate the change in the lipid clustering ability of C2 when the protein-protein interaction is -2.0 kcal/mol. In the snapshots for binding of C2 to 70:20:10 PC/PS/Chol with ω_a= -2.0 kcal/mol, it is apparent that when bound to the lattice, C2 forms tightly packed protein clusters (Figure 15 D). Very large PS/Chol domains correspond to these C2 clusters (Figure 15 C), thus accounting for the presence of very large PS domains. Where C2 proteins are not bound to the lattice, only very small PS domains are present. For binding of C2 to 70:20:10 PC/PS/Chol with ω_a= 0 kcal/mol, the protein snapshot shows that C2 does not form tightly packed clusters on the lattice (Figure 15 B). Many proteins segregate to regions of the lattice corresponding to large PS/Chol domains (Figure 15 A), while other proteins segregate into smaller groups which correspond to medium sized PS/Chol domains. Again, where there are no proteins bound, only very small PS domains are present. These snapshots demonstrate the broad

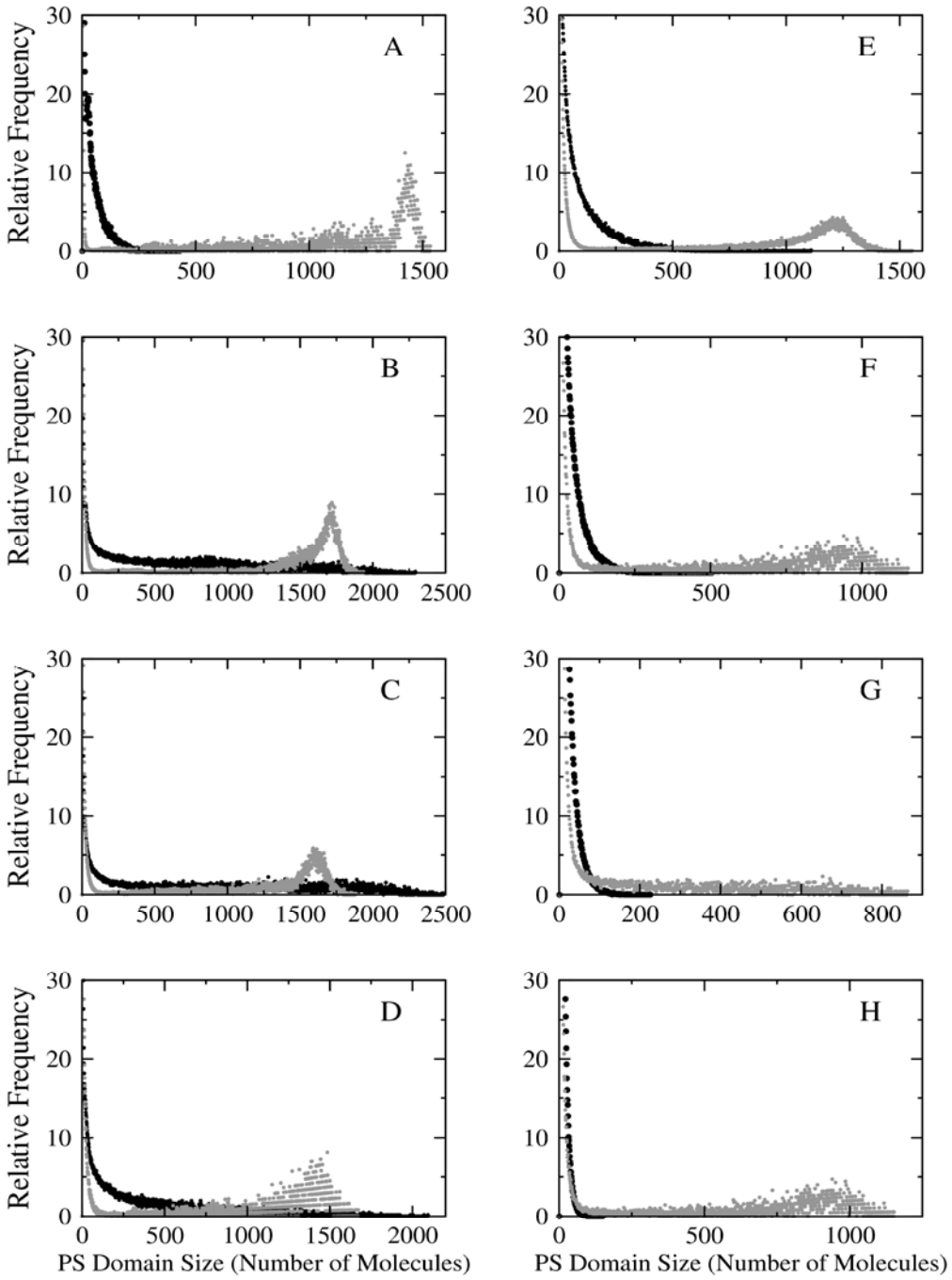

Figure 14. PS distribution for PC/PS/Chol mixtures containing 0 (A), 5 (B), 10 (C), 15 (D), 20 (E), 25 (F), 30 (G), and 35 (H) mol % Chol with ω_a= 0 kcal/mol (black) and ω_a= -2.0 kcal/mol (gray). All distribution plots are for binding of 100 C2 proteins.

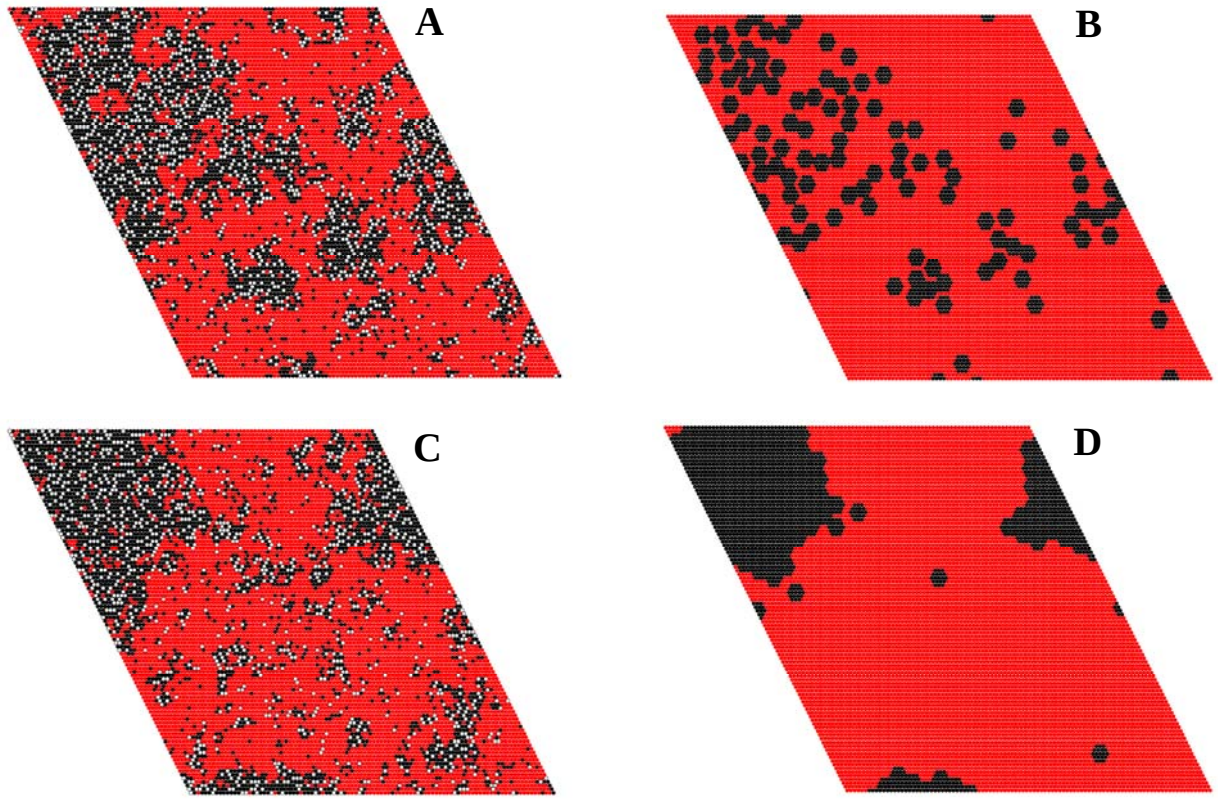

Figure 15. Bilayer and protein snapshots for 70:20:10 PC/PS/Chol mixture with ω_a= -2.0 kcal/mol (A, B) and ω_a= 0 kcal/mol (C, D) upon binding of 100 C2 proteins. In the protein snapshots (B, D) the large black hexagons represent individual C2 proteins. In the bilayer snapshots (A, C) PS molecules are in black, Chol molecules are white, and PC molecules are red.

range of PS domains formed when C2 binds with ω_a= 0 kcal/mol.

Cholesterol and Membrane Asymmetry. For simulations monitoring binding of proteins to bilayer mixtures of PC/PS/Chol, the ability of A5 and C2 to induce membrane asymmetry was analyzed. When incorporated into the bilayer, Chol is allowed to exchange sites with lipids on the opposite leaflet. This ability of Chol to flip from one leaflet to another allows for the study of membrane asymmetry induced by protein binding. Furthermore, exchange from one leaflet to another should only occur at sites where protein is bound, because of the favorable protein-lipid interaction between the protein and PS. For each simulation, the excess PS and Chol on the top leaflet with respect to total Chol mole fraction was monitored. Figure 16 shows that binding of A5 induced a maximum lipid excess of 8% for PS and 6% for Chol for mixtures containing 10 and 15 % Chol respectively when ω_a= 0 kcal/mol (top). The extent of bilayer asymmetry was relatively unaffected by the favorable protein-protein interaction (Figure 16, bottom).

For simulations of C2 binding with ω_a=0 kcal/mol, plotted results show a much broader range of maximum PS excess for simulations with ω_a= -2.0 kcal/mol, with a maximum PS excess (black) of approximately 22% for mixtures containing 5 to 25 mol % Chol (Figure 17). The maximum Chol excess (gray) was approximately 17% at 25 mol % Chol. For binding of C2 without the protein-protein interaction (ω_a= 0 kcal/mol)
the extent of membrane asymmetry decreases from 22% to 15% for PS and from 17% to 7% for Chol (Figure 17).

Dependence of FRET on Peptide Incorporation to POPC/BSM/Chol membranes

The dependence of energy transfer efficiency (E_t) between MB-POPE (donor) and NBD-POPE (acceptor) in the presence of a single α-helical peptide was examined. The transmembrane region of the linker for activation of T-cells (LAT), a peptide believed by some

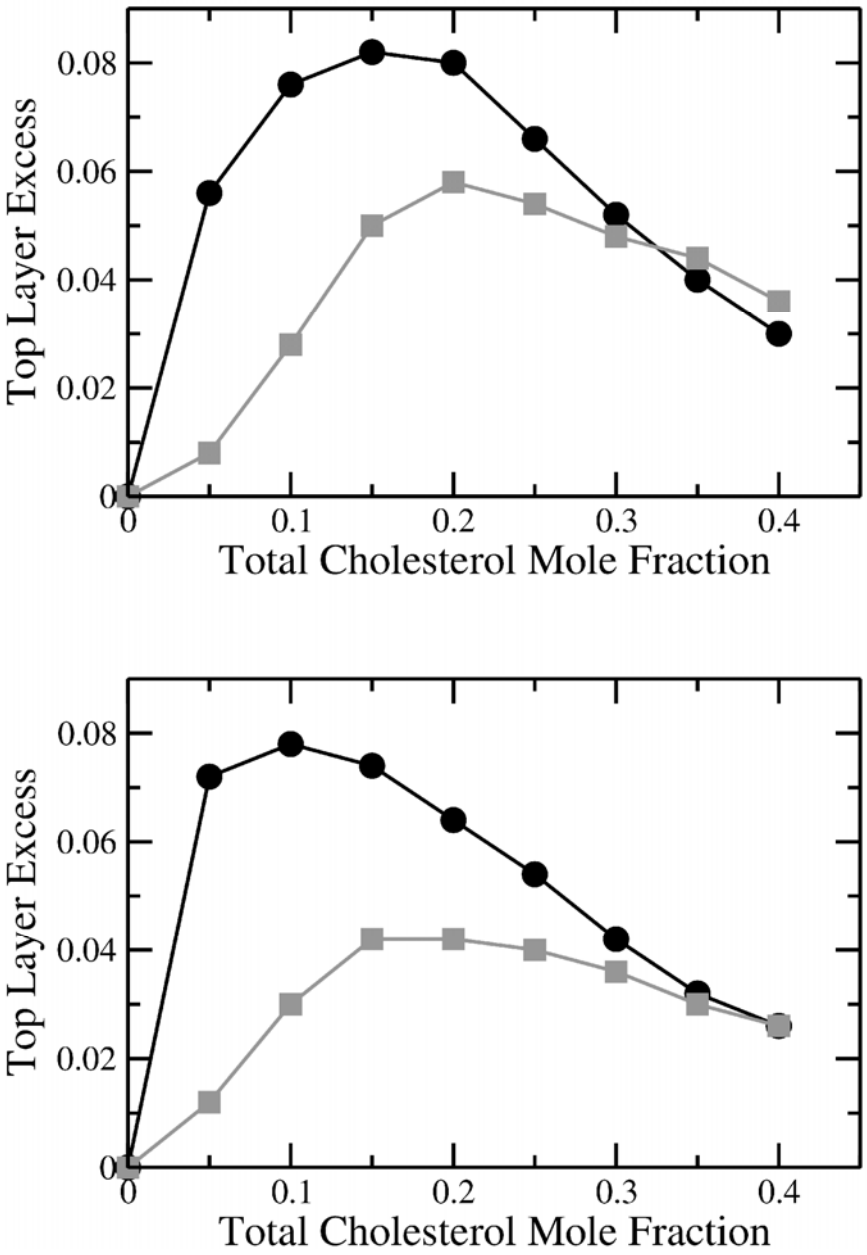

Figure 16. PS (black) and Chol (gray) top monolayer excess for A5 with ω_a= 0 kcal/mol (top) and ω_a= -2.0 kcal/mol (bottom).

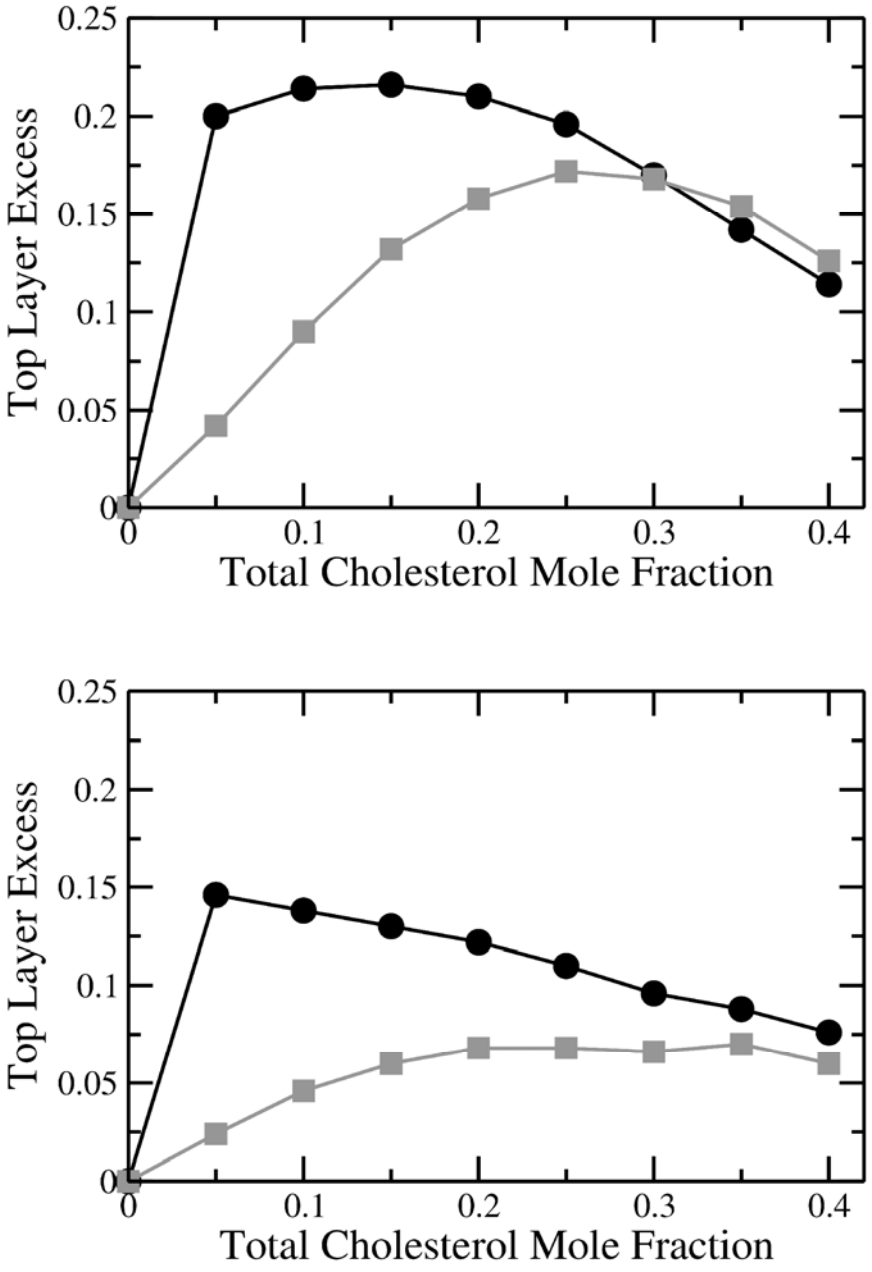

Figure 17. PS (black) and Chol (gray) top monolayer excess for C2 with ω_a= 0 kcal/mol (top) and ω_a= -2.0 kcal/mol (bottom).

associate with lipid rafts (13), was incorporated to POPC/BSM/Chol vesicles at 10 mol % of the total vesicle concentration and energy transfer efficiency was monitored. LAT was incorporated into lipid vesicles by mixing the desired molar amount of LAT (10 mol% for these experiments) in MeOH, with the desired molar amounts of all lipid species in $CHCl_3$.

To determine if peptide incorporation was successful, vesicles containing 90:10 POPC/LAT were prepared and emission spectra were collected from 300 to 500 nm and the emission maximum of the tryptophan of LAT was monitored. Fluorescence emission spectra were also collected for free LAT in solution and the results were compared (Figure 18). When excited at 280 nm, the emission maximum of the tryptophan residue shifted from 350 nm when in solution (black) to 320 nm when incorporated in 100 % POPC vesicles (gray). This shift in the emission maximum demonstrates that the peptide went from a polar environment, in aqueous solution, to a nonpolar environment in the bilayer, thus indicating that peptide insertion into LUVs was successful.

The dependence of energy transfer efficiency on the insertion of LAT in POPC/BSM/Chol membranes was measured using the following conditions. The concentration of MB-POPE was kept constant at 0.5 mol % of the total lipid and the mole fraction of POPC (X_{POPC}) was varied. The BSM/Chol content was kept at a 1:1 molar ratio and NBD/MB was kept at a 1.5:1 molar ratio for all vesicle compositions. A series of spectra were collected for vesicles containing 20 to 100 mol % POPC in the presence and absence of LAT, incorporated into the vesicles at 10 mol% relative to the total lipid.

Results from this series (Figure 19) show that addition of LAT into POPC/BSM/Chol mixtures causes a reduction in the energy transfer efficiency (E_t) between MB-POPE and NBD-POPE for all lipid compositions. This is apparent by the decrease in the intensity of the NBD

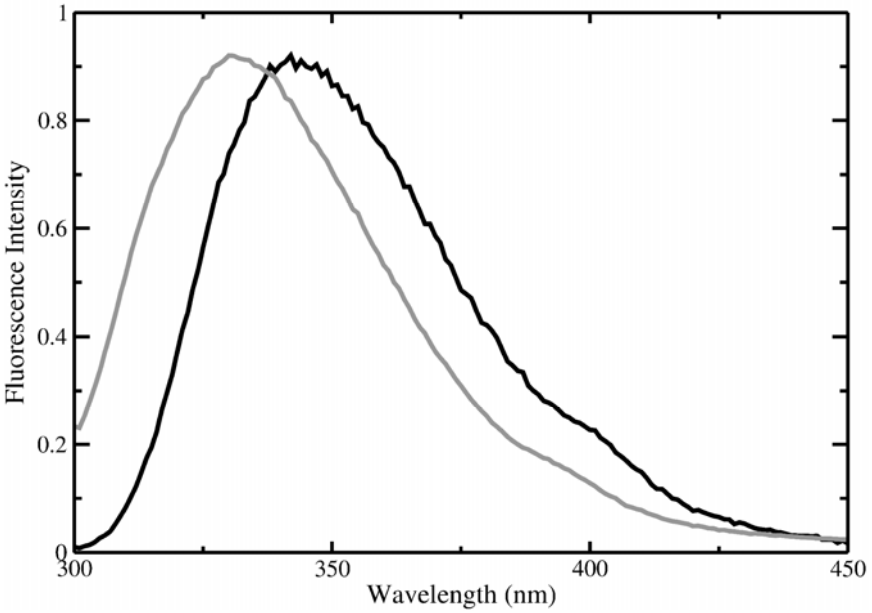

Figure 18. Tryptophan emission shift when excited at 280 nm. Black line is 1 μM LAT in solution; gray line is 10 μM LAT incorporated into of 100 μM POPC vesicles.

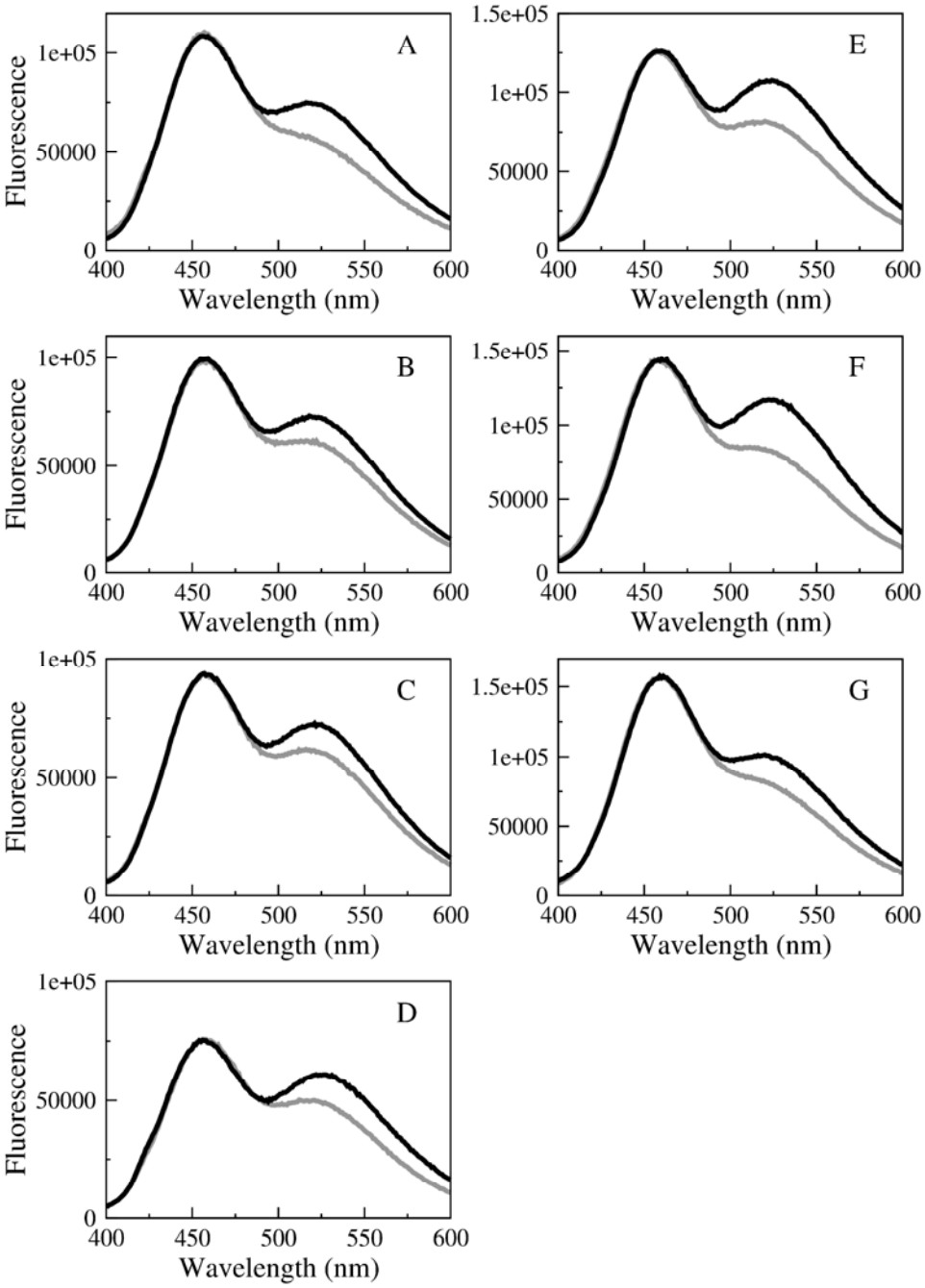

Figure 19. Representative series of spectra recorded where the POPC was varied in POPC:BSM:Chol mixtures. (*A*) X_{POPC}= 0.20, (*B*) 0.30, (*C*) 0.40, (*D*) 0.50, (*E*) 0.60, (*F*) 0.80, (*G*) 1.0. BSM/Chol ratio was kept at 1:1. MB-POPE and NBD-POPE were 0.5 mol % and 0.75 mol % respectively. Results for each mixture is shown in the presence (grey) and absence (black) of 10 mol % LAT. The total lipid concentrations are the same in all samples (100 μM).

peak at 524 nm for all samples containing 10 mol % LAT (gray) when compared to samples without LAT (black) in Figure 19. This suggests that insertion of LAT might change the lipid distribution, creating larger liquid-disordered (L_d) domains. Since E_t depends on donor/acceptor proximity, having MB and NBD in large L_d domains would increase the average distance between fluorophores, thus resulting in a decrease in E_t. Another possibility, however, is that LAT could be directly interacting with one of the fluorescent probes and possibly altering the emission of MB-POPE or NBD-POPE.

To determine the cause of the decrease in energy transfer efficiency between MB-POPE and NBD-POPE, POPC vesicles containing only 0.5 mol % MB-POPE or 0.75 mol % NBD-POPE were prepared in the presence and absence of 10 mol % LAT. For vesicles containing POPC and 0.5 mol % MB-POPE, the excitation wavelength was set at 367 nm and emission was scanned from 400 to 600 nm. For POPC vesicles containing 0.75 mol % NBD-POPE, the excitation wavelength was set at 463 nm and emission was scanned between 475 nm and 625 nm.

Results from these samples (Figure 20) show that addition of 10 mol % LAT to POPC vesicles containing 0.5 mol % MB-POPE does not affect the intensity of the emission maximum of MB-POPE at 457 nm. However, for the POPC vesicles containing 0.75 mol % NBD-POPE, the intensity of the emission maximum of NBD-POPE at 524 nm is shown to decrease by a factor of 1.28 upon addition of 10 mol % LAT (gray) when compared to NBD-POPE emission in the absence of LAT (black). These results indicate that incorporation of LAT into lipid vesicles may suppress the emission of NBD-POPE but not affect the fluorescence of MB-POPE.

To account for this possible interaction between LAT and NBD-POPE, calculated values for E_t in the presence of 10 mol % LAT were corrected for the overall decrease in NBD-POPE fluorescence caused by the peptide (Figure 21). The corrected E_t data was plotted against E_t data for vesicles without peptide and can be seen in Figure 22. In both data sets E_t goes through a

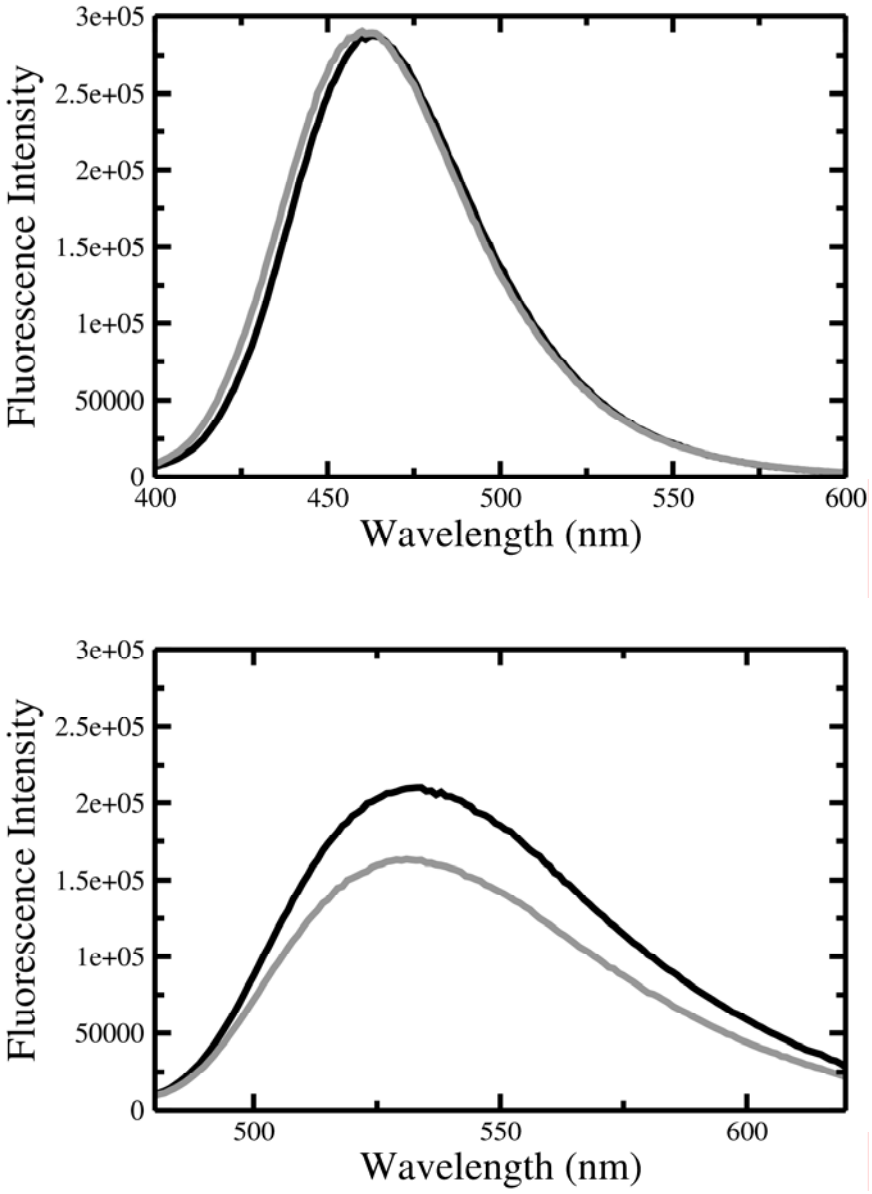

Figure 20. Individual fluorescence spectra for 0.5 mol % MB-POPE (top) and 0.75 mol % NBD-POPE (bottom), both in the presence (grey) and absence (black) of 10 mol % LAT. Vesicle composition for all samples is 100 mol % POPC. The total lipid concentrations are the same in all samples (100 μM).

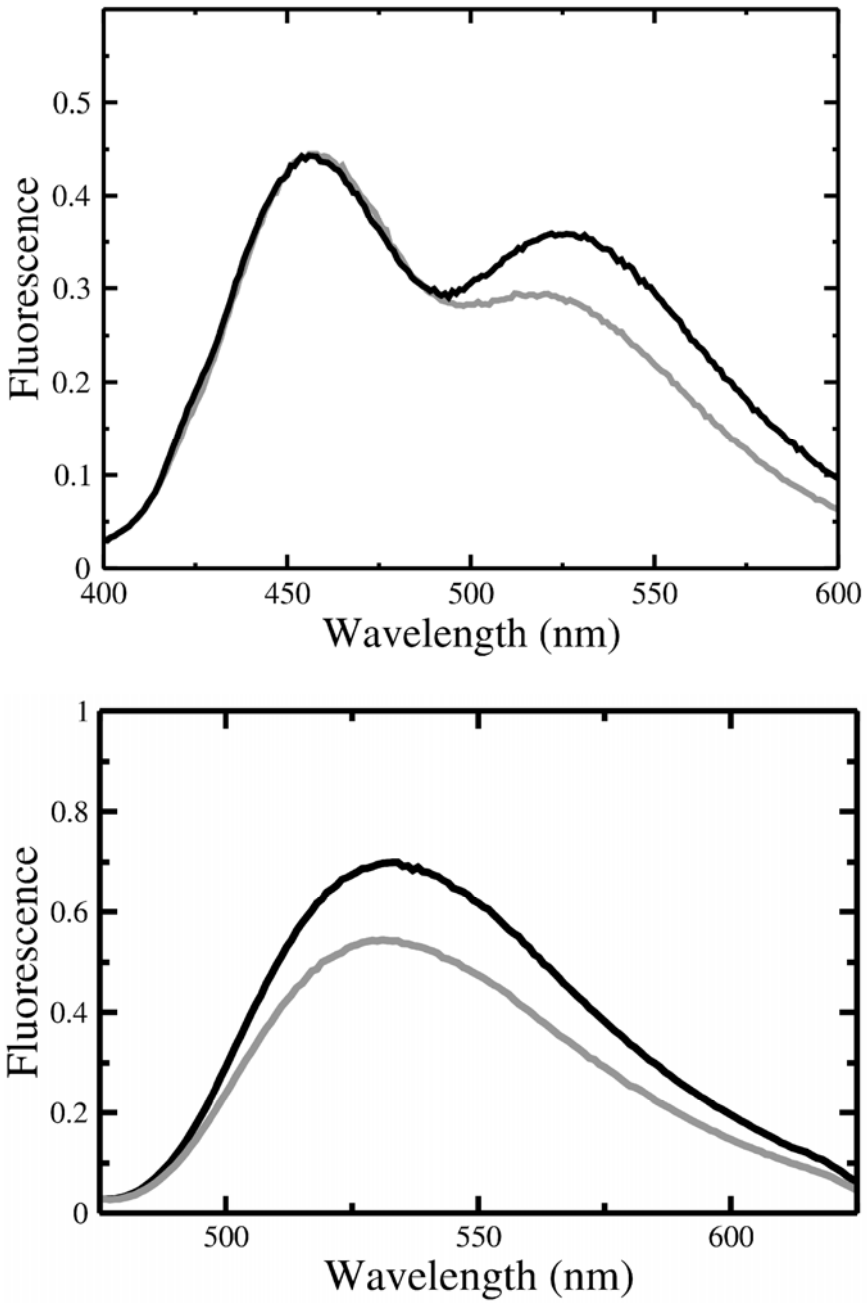

Figure 21. Energy transfer between MB-POPE and NBD-POPE in 50:25:25 POPC/BSM/Chol (top) and emission spectra of NBD-POPE (bottom) in the presence (gray) and absence (black) of 10 mol% LAT (top). Vesicle concentration for all mixtures is 100 μM.

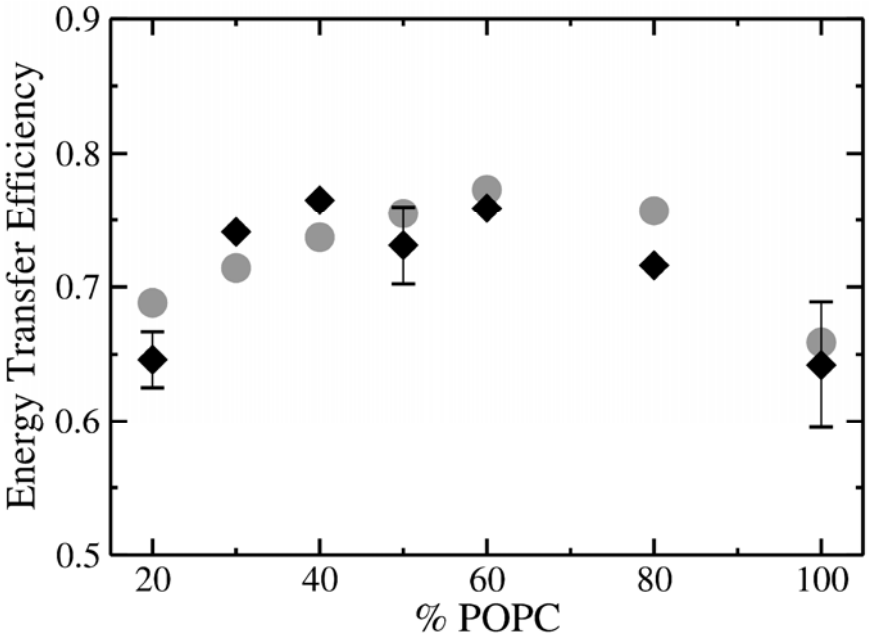

Figure 22. Normalized energy transfer efficiency for samples containing 20 to 100 mol % POPC, 1:1 BSM/Chol, 0.5 mol % MB-POPE, and 0.75 mol % NBD-POPE. Results are shown in the presence (black diamond) and absence (grey circle) of 10 mol % LAT. The total lipid concentration is the same in all samples (100 μM).

maximum when the POPC mole fraction is approximately 0.60. This maximum E_t is approximately 0.75 for vesicles containing 10 mol % LAT (black) and vesicles without peptide inserted (gray). The dependence of E_t on the mole fraction of POPC indicates that lipid domains exist in each system. The identical trend in E_t for both systems indicates that the addition of LAT to POPC/BSM/Chol mixtures does not affect the energy transfer efficiency between the fluorescent probes MB and NBD, and thus, insertion of LAT into these systems does not affect lipid distribution.

Experiments were conducted to determine if LAT inserts into specific lipid regions, L_d or L_o, or inserts into membranes uniformly and without preference for specific domains. To investigate this, vesicles were prepared with the fluorescent probe 7-methoxy-coumarin-POPE (7-MC-POPE). When tryptophan is excited at 280 nm, 7-MC accepts this energy and emits at 396 nm. This makes the tryptophan residue of LAT (donor) and 7-MC-POPE (acceptor) a good Förster energy transfer pair. Energy transfer between tryptophan and 7-MC-POPE (Figure 23) was monitored for 100 % POPC vesicles (black) and 50:25:25 POPC/BSM/Chol vesicles (gray). Results from these experiments show that the E_t between tryptophan and 7-MC is unaffected by the presence of both ordered and disordered domains. This indicates that LAT inserts into POPC/BSM/Chol membranes in a manner that is nonspecific to lipid composition. That is, LAT shows no preference between L_d and L_o domains.

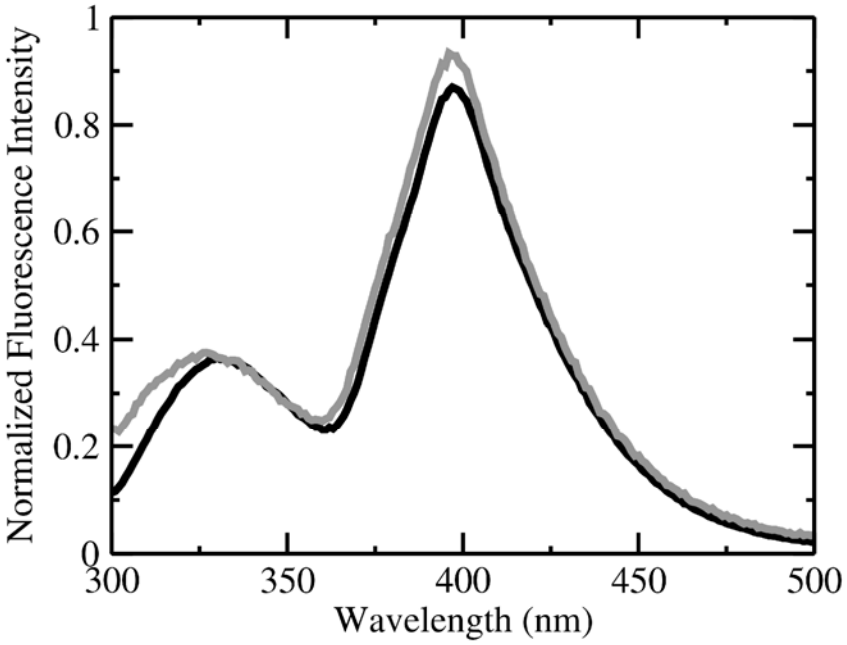

Figure 23. Tryptophan energy transfer to 7-methoxy coumarin when excited at 280 nm. Black line is 100 μM POPC vesicles; gray line is 100 μM 50:25:25 POPC/BSM/Chol vesicles. All samples contain 2 mol % 7-MC-POPE and 10 mol % LAT.

DISCUSSION

Lipid Domain Regulation and Protein Binding

This study focused on monitoring the ability of annexin A5 to induce lipid domain formation upon binding to mixed model membranes. While A5 has been found to play a role in several biological processes such as exocytosis and endocytosis, how it interacts with the bilayer has remained uncertain. It is known that A5 binds to negatively charged lipids in a Ca^{2+}-dependent manner. Also, it has been shown that when bound to negatively charged membranes, A5 will group into trimer clusters, thus indicating that individual A5 proteins may interact favorably with one another (10, 11). It is these properties which have lead to the hypothesis that binding of A5 may result in the formation of lipid domains mediated by the thermodynamic coupling of favorable protein-lipid, protein-protein, and unlike lipid interactions. This hypothesis was tested using Monte Carlo computer simulations of simple model systems that were mixtures of PS, PC, and Chol lipids.

All Monte Carlo simulations were performed using experimentally determined protein-lipid binding constants to ensure that the simulations were relevant to experimental conditions (12). Initial simulations were performed to determine general binding of A5 to the membrane (G_{off}) and the preferential protein-lipid interaction (ω_p) by using experimentally determined protein binding constants. The G_{off} and ω_p for annexin A5 in the presence of 20 μM Ca^{2+} were found to be -7.60 kcal/mol and -162 cal/mol respectively. For simulations monitoring binding of A5 in the presence of Ca^{2+}, the G_{off} and ω_p were set to these values.

PC/PS Mixtures and Protein Binding. Binding of A5 to anionic lipids is mediated by the presence of Ca^{2+}; therefore, the presence of Ca^{2+} in the simulations was expected to increase the size of PS domains upon A5 binding. However, simulations show that the addition of A5 to

various PC/PS mixtures in the presence of Ca^{2+} does not induce lipid demixing (Figure 5, gray). This indicates that while A5 interacts favorably with negatively charged lipids such as PS in the presence of Ca^{2+}, the magnitude of this interaction (ω_p= -156 cal/mol) is not large enough to induce the formation of PS domains upon binding in the presence of Ca^{2+}.

Binding studies of annexin A5 indicate that A5 may form protein clusters upon binding to membranes (10). A favorable protein-protein interaction parameter (ω_a= -2.0 kcal/mol) was added to simulate protein clustering on the lattice surface. Simulations of A5 on binary systems of PC/PS show little increase in PS cluster size when ω_a= -2.0 kcal/mol when compared to A5 binding when ω_a= 0 kcal/mol (Figure 6). This is further verified by representative simulation snapshots of A5 binding with ω_a = -2.0 kcal/mol (Figure 7 C, D) and ω_a = 0 kcal/mol (Figure 7 A, B). These snapshots clearly illustrate that clustering of A5 on the bilayer surface (Figure 7 D) does not alter the lipid distribution (Figure 7 C) in the bilayer. Therefore, binding of A5 to PS/PC membranes in the presence of Ca^{2+} does not induce lipid domain formation for such mixtures.

Monte Carlo simulations were performed to monitor the effect of a favorable protein-protein interaction (ω_a= -2.0 kcal/mol) for the C2 motif of rat synaptotagmin I. Like annexin, the C2 motif binds to negatively charged lipids in a Ca^{2+} dependent manner. C2 has been extensively studied can induce the formation of anionic lipid domains upon binding to mixed model systems of PS and PC (4). Previous research determined the G_{off} and ω_p for C2 to be -5 kcal/mol and -1000 cal/mol respectively. While the protein binding free energy to PC for C2 is very similar to that of A5, its protein-PS interaction is much stronger and more favorable than that of A5.

Data for 80:20 PC/PS shows that in the absence of protein-protein interactions (ω_a= 0 kcal/mol), binding of C2 to the bilayer induces the formation of PS domains, and the lipid domain size increases with increasing protein concentration (Figure 8, top). When the favorable

protein-protein interaction (ω_a= -2.0 kcal/mol) was added, the average lipid domain size was unaffected at lower protein concentration (20 to 60 proteins) while it increased to from 10 to 16 lipids in the presence of 100 C2 (Figure 8 top). These results indicate that for protein binding to induce the formation of lipid domains in binary systems of PS and PC, the favorable protein-PS interaction must be much larger than a few hundred calories per mole (but approximately -1 kcal/mol). Unlike that of A5, coupling of the very favorable protein-PS interaction of C2 with a strong protein-protein interaction of -2.0 kcal/mol does cause an increase in lipid domain size upon protein binding. Bilayer and protein snapshots from simulations with ω_a= -2.0 kcal/mol (Figure 9 C, D) clearly illustrate how C2 clustering on the bilayer surface results in large PS domains directly corresponding to the large protein clusters.

PC/PS/Chol Mixtures and Protein Binding. Monte Carlo simulations were performed to monitor protein binding to PS in the presence of cholesterol. Cholesterol can form condensed complexes with PS in the bilayer (21). The ability of these two lipid species to form a complex may have an effect on the ability of both A5 and C2 to induce lipid domain formation as well as induce membrane asymmetry. Additional unlike lipid interactions will couple with all other unlike lipid and protein-lipid interactions for protein binding to PC/PS mixtures, and thereby possibly lead to the formation of larger lipid domains upon protein binding. Typically, unlike lipid interactions are a few hundred calories per mole, and the value for ω_{DS} (interaction between Chol and PS) was chosen to be -250 cal/mol to indicate a favorable interaction between the lipid species.

The effect of A5 binding to PC/PS/Chol mixtures was monitored in the presence of 20 μM Ca^{2+} for systems containing 5 to 40 mol % Chol and PS content was kept at 20 mol %. The results showed that addition of A5 to PC/PS/Chol systems does induce lipid demixing (Figure 10). A maximum average PS domain size was observed for mixtures containing 10 mol % Chol

for binding of A5 without the favorable protein-protein interaction (ω_a= 0 kca/mol). This maximum corresponds to the 2:1 ratio of PS/Chol lipids within the system when the bilayer composition is 70:20:10 PC/PS/Chol. At 10 mol % Chol, a maximum number of PS lipids can interact with Chol and A5 in a cooperative manner. At higher Chol concentrations (40 mol %) many more Chol molecules are present than PS molecules, allowing fewer PS molecules to interact with a single Chol, thus resulting in smaller PS-Chol clusters. At lower Chol concentrations, there is an excess PS content with respect to Chol. Therefore not all PS lipids will be able to interact with Chol resulting in a decrease in PS clustering.

Again, simulations were performed to monitor the effect of the favorable protein-protein interaction of -2.0 kcal/mol. These simulations show an increase in the maximum PS domain size upon A5 binding. The maximum average domain size increased (purple) and was again present at 10 mol % Chol (Figure 10). Protein and bilayer snapshots for A5 with ω_a= 0 kcal/mol (Figure 11 A, B) show that A5 does not cluster on the bilayer surface when bound, which results in the presence of many small to medium PS/Chol domains. The PS distribution for A5 with ω_a= 0 kcal/mol illustrates the presence of only many small PS domains and medium PS domains, with very few larger domains (Figure 12, green). Protein and bilayer snapshots for A5 with ω_a= -2.0 kcal/mol (Figure 11 C, D) show that with the favorable protein-protein interaction, A5 forms many large clusters when bound to the bilayer surface. This protein clustering results in the presence of large PS/Chol domains directly corresponding to the protein cluster. Where proteins are not bound to the lattice, only small PS domains are present. Figure 12 shows the PS distribution for these simulations (purple). It is apparent that the ability of A5 to form large lipid domains in PC/PS/Chol bilayers depends on protein clustering. The net strength of the protein-PS interaction is amplified in large protein clusters. Since the preferential protein-PS interaction for A5 is very weak, protein clustering on the bilayer surface overcomes this weak interaction,

thus resulting in the presence of large PS domains.

The effect of C2 binding to PC/PS/Chol mixtures was also monitored for systems containing 5 to 40 mol % Chol and keeping PS content at a constant 20 mol %. Binding of C2 to PC/PS mixtures has already been shown to induce the formation of PS clusters (Figure 9). Addition of cholesterol with its favorable interaction with PS was expected to greatly increase the extent of lipid demixing upon binding of C2. Simulations monitoring binding of C2 to PC/PS/Chol mixtures with ω_a= 0 kca/mol show that binding of C2 induces much large PS domains than binding of A5, with a maximum average PS domain size of approximately 23 lipids for mixtures containing 10 mol % Chol (Figure 13, green). Again, this maximum at 10 mol % Chol corresponds to the 2:1 ratio of PS/Chol within the system. Inclusion of the favorable protein-protein interaction (Figure 13 purple) in these simulations resulted in a decrease in the average PS domain size (15 lipids).

Investigation of PS distribution for all mixtures with ω_a= -2.0 kcal/mol revealed that binding of C2 induces the formation of many small PS domains and may large PS domains (at least 1000 PS molecules) for mixtures containing 0 to 25 mol % Chol (Figure 14, gray, A-E,). Snapshots of C2 binding with ω_a= 0 kcal/mol show the presence of many large, medium, and small PS domains (Figure 15 A, B). When ω_a= -2.0 kcal/mol, relatively all C2 proteins cluster with one another on the bilayer when bound (Figure 15 C), with large PS domains correspond to the C2 clusters (Figure 15 D). Where proteins are not bound, only very small PS domains are observed, thus, resulting in the bimodal distribution of PS domains observed in Figure 14 (gray). Unlike A5, binding of C2 can induce the formation of large lipid domains in PC/PS/Col mixtures without the favorable protein-protein interaction of -2.0 kcal/mol. However, addition of this favorable interaction causes an increase in the number of large PS domains when compared to C2 binding without this interaction.

Cholesterol and Membrane Asymmetry. For Monte Carlo simulations of protein binding to PC/PS/Chol bilayers, Chol molecules were allowed to switch places with lipid molecules on the opposite leaflet. This allows lipids to flip between the inner or outer monolayer throughout the simulations of bilayers containing PC/PS/Chol. Binding of A5 to PC/PS/Chol mixtures results in a shift in PS and Chol distribution, creating an excess of both lipid species on the outer leaflet, where A5 is bound (Figure 16). The maximum top layer excess for PS was present for mixtures containing 15 mol % Chol while the maximum Chol excess was at 20 mol % Chol (Figure 16, top). The presence of favorable protein-protein interaction (ω_a= -2.0 kcal/mol) did not affect the extent of lipid demixing upon binding of A5 (Figure 16, bottom). While the A5-PS interaction may be weak, the interaction is still strong enough to induce bilayer asymmetry upon binding to PC/PS/Chol mixtures. The ability of Chol to flip between layers allowed the favorable interaction between A5 and PS to cause the exchange of Chol on the outer leaflet with PS on the inner leaflet where A5 was bound to the lattice surface. When the concentration of PS is greater on the outer leaflet, this also causes Chol to flip to the outer layer as well (exchange with PC). Therefore, addition of A5 to mixtures of PC/PS/Chol can induce membrane asymmetry even if A5 does not directly interact with some of the lipids, such as cholesterol.

Membrane asymmetry was also monitored for the binding of C2 to PC/PS/Chol systems. Results from these simulations showed that binding of C2 to PC/PS/Chol mixtures in the presence of Ca^{2+} caused a much larger shift in membrane asymmetry when compared to binding of A5 (Figure 17, top). Also, the maximum PS top layer excess spanned a much broader range of bilayer mixtures (5 to 25 mol % Chol). This is the result of the much more favorable protein-PS interaction for C2 (-1000 kcal/mol) than that of A5 (-156 kcal/mol). Incorporation of the favorable protein-protein interaction for C2 caused a reduction in membrane asymmetry (Figure 17, bottom) when compared to binding of C2 with ω_a= 0 kcal/mol. When the protein-protein

interaction was 0 kcal/mol, C2 bound to the lattice without clustering (Figure 15 B). However, when the protein-protein interaction was -2.0 kcal/mol, C2 formed very tightly packed clusters on the lattice surface (Figure 15 D). The ability of PS to exchange sites with Chol is dependent on protein contact with the exchange site. Therefore, when the proteins are confined to a tightly packed cluster, each protein is in contact with fewer lipid molecules than a single protein bound to the lattice. This explains the decrease in membrane asymmetry for both PS and Chol when C2 clusters on the lattice surface (ω_a = -2.0 kcal/mol).

Peptide insertion and Lipid Domains

This part of the research was aimed at determining how incorporation of an α-helical peptide into model membranes affects lipid distribution in POPC/BSM/Chol systems. This was monitored by fluorescence resonance energy transfer (FRET) between a designated acceptor/donor pair. The acyl chains of these fluorescent probes are identical to that of POPC, therefore they are expected to partition into the liquid-disordered (L_d) phase composed of POPC. For all experiments, the POPC mole fraction was varied from 20 to 100 mol % in the presence and absence of LAT, and FRET between MB-POPE and NBD-POPE was monitored. An analogue of the transmembrane region of LAT was chosen for membrane incorporation because LAT is believed by some to associate with lipid rafts (13).

FRET experiments for mixtures of POPC/BSM/Chol showed that incorporation of LAT into mixed model systems decreases the observed energy transfer between the fluorescent probes MB-POPE and NBD-POPE for all mixtures (Figure 19). This was indicated by the decrease in intensity of the NBD peak at 524 nm for all samples containing LAT when compared to mixtures without LAT. However, it was determined that this decrease in NBD emission was only the result of a peptide-NBD interaction (Figure 21). Therefore, insertion of LAT into

POPC/BSM/Chol membranes does not affect the extent of energy transfer between MB and NBD, and incorporation of LAT does not change the size of lipid domains within each vesicle system. LAT does not seem to interact with any of the lipid species in POPC/BSM/Chol bilayers strongly enough to either further increase or decrease the size of lipid domains within these systems.

The preference of LAT for liquid-ordered (L_o) and liquid-disordered (L_d) domains was aslo investigated using FRET experiments between the tryptophan residue of LAT and 7MC-POPE. Like MB-POPE and NBD-POPE, the acyl chains of 7MC-POPE are identical to that of POPC, therefore it is expected to partition into the L_d phase composed of POPC. Figure 23 shows that the E_t between tryptophan and 7-MC was unaffected by the presence of L_d and L_o domains in 50:25:25 POPC/BSM/Chol vesicles (gray) when compared to 100 % POPC vesicles (black).

While it has been speculated that LAT must associate with lipid rafts in order to function, insertion of the transmembrane peptide of LAT into these tightly packed phases would be difficult because of the high degree of order within these domains. The results from FRET experiments using the acceptor/donor pair Trp and 7-MC indicate that while the function of LAT may be dependent on the presence of lipid rafts, the transmembrane peptide of LAT does not preferentially associate with these domains. Partitioning of LAT into the ordered phase would have resulted in an increase in energy transfer between the Trp of the peptide and 7MC-POPE because of the increase in proximity of the fluorphores. Energy transfer efficiency between this acceptor/donor pair was unaffected by insertion of LAT into the bilayer, indicating that LAT may insert into both ordered and disordered phases.

References

1. Edidin, M. (2003) The state of lipid rafts: from model membranes to cells. *Annu. Rev. Biophys. Biomol. Struct. 32*, 257-283.

2. Brown, D. A., and London, E. (1998) Functions of lipid rafts in biological membranes. *Ann. Rev. Cell Dev. Biol. 14*, 111-136.

3. Simons, K. and Ikonen, E. (1997) Functional rafts in cell membranes. *Nature 387*, 569-572.

4. Hinderliter, A., Almeida, P. F. F., Creutz, C. E., Biltonen, R. L. (2001) Domain formation in a fluid mixed lipid bilayer modulated through binding of the C2 protein motif. *Biochemistry 40*, 4181-4191.

5. Frazier, M. L., Wright, J. R., Pokorny A., Almeida, P. F. F. (2007) Investigation of domain formation in sphingomyelin/cholesterol/POPC mixtures by fluorescence resonance energy transfer and monte carlo simulations. *Biophys. J.* 92:2422-2433.

6. Sugar, I. P., Thompson, T. E., and Biltonen, R. L. (1999) Monte Carlo simulation of two-component bilayers: DMPC/DSPC mixtures. *Biophys. J. 76*, 2099-2100.

7. Jerala, R., Almeida, P. F. F., and Biltonen, R. L. (1996) Simulation of the gel-fluid transition in a membrane composed of lipids with two connected acyl chains: application of a dimer-move step. *Biophys. J. 71*, 609-615.

8. Raynal, P., and Pollard, H. B. (1994) Annexins: the problem of assessing the biological role for a gene family of multifunctional calcium- and phospholipid-binding proteins. *Biochim. Biophys. Acta 1197*, 63-93.

9. Gerke, V., Creutz, C. E., and Moss, S. E. (2005) Annexins: linking Ca^{2+} signalling to membrane dynamics. *Nat. Rev. 6*, 449-461.

10. Mo, Y., Campos, B., Mealy, T. R., Commodore, L., Head J. F., Dedman, J. R., and Seaton, B. (2003) Interfacial basic cluster in annexin V couples phospholipid binding and trimer formation on membrane surfaces. *J. Biol. Chem. 278*, 2437-2443.

11. Oling, F., Bergsma-Schutter, W., and Brisson, A. (2001) Trimes, dimers of trimers, and trimers of trimers are common building blocks of annexin A5 two-dimensional crystals. *J. Struct. Biol. 133*, 55-63.

12. Almeida, P. F. F., Sohma, H., Rasch, K. A., Wieser, C. M., Hinderliter, A. (2005) Allosterism in membrane binding: a common motif of the annexins? *Biochemistry 44*, 10905-10913.

13. Shogomori, H., Hammond, A. T., Ostermeyer-Fay, A. G., Barr, D. J., Feigenson, G. W., London, E., Brown, D. A. (2005) Palmitoylation and intracellular domain interactions both contribute to raft targeting of linker for activation of T cells. *J. Biol. Chem. 280*, 18931-18942.

14. Zhang, W., Sloan-Lancaster, J., Kitchen, J., Trible, R. P., and Samelson, L. E. (1998) LAT: the ZAP-70 tyrosine kinase substrate that links T cell receptor to cellular activation. *Cell 92*, 83-92.

15. Bartlett, G. R. (1959) Phosphorous assay in column chromatography. *J. Biol. Chem. 234*, 466-468.

16. Pokorny, A., Birkbek, T. H., and P. F. F. Almeida, P. F. F. (2002) Mechanism and kinetics of δ-lysin interaction with phospholipid vesicles. *Biochemistry*. *41*, 11044-11056.

17. Metropolis, N., Rosenbluth, A. W., Rosenbluth, W. N., Teller, A. H., and Teller E. (1953) Equation of state calculations by fast computing machines. *J. Chem. Phys. 21*, 1087-1092.

18. Binder, K., and Heermann, D. W. (1997) Monte Carlo simulation in statistical physics. *Solid-State Sciences*, 3rd ed., Springer, New York.

19. Almeida, P. F. F., Pokorny, A., Hinderliter, A. (2005) Thermodynamics of membrane domains. *Biochim. Biophys. Acta* 1720, 1-13.

20. Huang, J., Swanson, J. E., Dibble, A. R. G., Hinderliter, A. K., and Feigenson, G. W. (1993) Nonideal mixing of phosphatidylserine and phosphatidylcholine in the fluid lamellar phase. *Biochemistry 26*, 2991-2997.

21. Radhakrishnan, A. and McConnell, H. M. (2000) Chemical activity of Cholesterol in Membranes. *Biochemistry 39*, 8119-8124.